UNIVERSITÀ POLITECNICA DELLE MARCHE

FACOLTÀ DI INGEGNERIA

Master Degree in Biomedical Engineering

Relationship between heart-rate variability and glycemia

Supervisor:

Prof. Laura Burattini

Co-supervisor:

Dr. Micaela Morettini

Dr. Andrea Tura

Student:

Francesca Vita

Academic Year 2020/2021

Abstract

Both heart-rate variability (HRV) and blood glucose levels are important information for assessing the individual's state of health. The aim of the present study is to assess the relationship that exists between HRV computed in 5-minutes intervals and glycemia values in the same 5-minutes intervals, in a population of subjects affected by type 1 diabetes mellitus while carrying out activities of daily living. The cardiovascular system ensures blood flow to all organs of the body through the heart, which acts as a muscle pump, and the vessels, which form a blood distribution network. The electrocardiogram (ECG) is a diagnostic tool used in clinical practice to record electrical heart activity. HRV is the measure of the time variation in R–R intervals during sinus arrhythmia, denoted as “N–N” intervals; it represents the influence of the autonomic nervous system on the sinoatrial (SA) node. While the activity of the parasympathetic nervous system increases HRV, the activity of the sympathetic nervous system decreases it. The time domain estimates of HRV that are more commonly used are: the standard deviation of all NN intervals (SDNN), the root mean square of successive NN interval differences (RMSSD), the heart rate (HR), the HRV triangular index (TRI), the triangular interpolation of the NN interval histogram (TINN), Approximate Entropy (ApEn), the ratio of successive NN intervals whose difference is > 50ms (NN50), the ratio between NN50 and all NN in the defined time period (pNN50), the measure of the standard deviation of instantaneous RR interval variability derived from the RR Poincarè plot (SD1), the measure of the continuous long-term RR interval variability derived from the RR Poincarè plot (SD2), and the ratio SD1/SD2. HRV frequency domain features are the power of high frequency (HF) component of HRV, the power of low frequency (LF) component of HRV, and the ratio LF/HF. All these HRV estimates could give information on the body's ability to regulate blood glucose levels and on the trend of the glycemic profile. Glucose is the primary source of energy of the cells of the human body and glycemia is regulated mainly by two hormones: insulin and glucagon. Insulin decreases glycemia while glucagon increases glycemia; the sympathetic nervous system stimulates glucagon secretion and suppress insulin secretion, increasing glycemia. Diabetes mellitus is a metabolic disease characterized by elevated blood glucose levels due to defects affecting insulin secretion, its action or both. Two categories of diabetes mellitus can be distinguished: type 1 and type 2. Continuous glucose monitoring (CGM) is a fairly recent technology that allows the continuous measurement of glucose levels (circa 300 measurements

in a day) in the interstitial fluid. There is some evidence in literature about the correlation between HRV and glycemia, but these studies were performed on data acquired in a controlled environment, during night, and using a limited number of glucose measurements so they do not reflect the relationship between HRV and blood glucose in everyday life conditions. In the present study the dataset used is publicly available and composed of 9 patients with type 1 diabetes mellitus; they were monitored with the wearable device Zephyr BioHarness3.0 for ECG recording and with iPro2 CGM system for glycemia measurements for four days in everyday life conditions. The ECG signals were visually analyzed with MATLAB R2020a and classified as having at least 5 consecutive minutes of ECG uninterrupted by noise or not. Also, CGM data were incomplete or lacking in some of the four days. Then the analysis was restricted to the subjects presenting at least one day with both glycemic tracing and ECG recording and not only noise. For the subjects presenting more than one day with both glycemic tracings and ECG recording, was selected the day with the highest number of ECG segments without noise and the highest number of CGM data. Then all the 5-minutes ECG segments in which the ECG was visible and suitable for the calculation of the HRV parameters were given in input to the HRVTool, a software developed as a Matlab Graphical User Interface to compute a list of HRV parameters. The Pearson's correlation coefficient (r) was used to study the strength of the correlation between each HRV parameter obtained and the glycemia value recorded in the same 5 minutes in each subject and considering all the subjects grouped. Statistical significance was set at $p<0.05$. Considering all the subjects grouped, weak but significant correlations were highlighted between glycemia and: SD1/SD2 ($r = -0.1883$, $p = 0.0009$), LF power ($r = 0.1962$, $p = 0.0005$), HF power ($r = -0.1962$, $p = 0.0005$), LF/HF ($r = 0.1617$, $p = 0.0045$), and HR ($r = -0.2966$, $p = 0.0000$). The non-significant correlations found were between glycemia and: SDNN ($r = 0.0738$, $p = 0.1971$), RMSSD ($r = -0.0619$, $p = 0.2800$), pNN50 ($r = -0.0130$, $p = 0.8206$), TRI ($r = 0.0901$, $p = 0.1150$), TINN ($r = 0.1002$, $p = 0.0796$), ApEn ($r = -0.0395$, $p = 0.4899$), SD1 ($r = -0.0619$, $p = 0.2798$), and SD2 ($r = 0.0968$, $p = 0.0904$). In conclusion, from this study it emerges the existence of weak correlations between HRV parameters computed in 5-minutes intervals and glycemia values in the same 5-minutes intervals in a population of subjects affected by type 1 diabetes mellitus while carrying out activities of daily living. Although the correlations found are not strong and only some are significant, this study may represent a starting point that paves the way for possible future studies aiming at estimate glycemia values from HRV obtained from the ECG recorded through non-invasive wearable sensors.

Index

Introduction

A close link is observed between the heart and the energy metabolism. Both heart rate (HR) and blood glucose levels are influenced by the two branches of the autonomic nervous system, the sympathetic and the parasympathetic. While the sympathetic nervous system increases both HR and glycemia, the parasympathetic nervous system decreases them. A non-invasive marker of the activity of the autonomic nervous system on the heart is the heart rate variability (HRV), the physiological phenomenon of the variation of the time interval between consecutive heart beats. A healthy heart does not beat evenly but presents high HRV, while reduced HRV is associated with myocardial infarction, diabetic neuropathy, and heart failure. HRV decreases during stress, when elevated sympathetic activity helps the body keep up with demand. In a normal situation, HRV increases during relaxing activities, when it dominates the parasympathetic nervous system. It would be of great interest to assess the relationship between HRV and glycemia because, if it is studied in every-day life conditions, it could be exploited to assess the glycemic value without the use of invasive methods such as the glucometer or minimally invasive methods such as continuous glucose monitoring (CGM), but directly from HRV obtained from the electrocardiogram (ECG) recorded through non-invasive wearable sensors. This would represent a great step forward in improving the living conditions of diabetic patients. There are some evidences in literature about the correlation between HRV and glycemia but these studies are performed on data acquired in a controlled environment such as a hospital, during night, and using a limited number of glucose measurements; some studies uses only one glycemia measure to define if the subject is healthy, or presents diabetes or if it is in a condition of impaired fasting glucose, without making a comparison between HRV and glycemia values acquired at the same time; other studies focus on subjects with type 2 diabetes and the computation of HRV parameters is performed only on limited periods, and some studies consider only a little number of HRV parameters. Therefore, these studies do not reflect the relationship between HRV and blood glucose in everyday life conditions. An analysis of the relationship between HRV and glycemia performed in everyday life conditions, on a population of subjects affected by type 1 diabetes mellitus monitored for entire days with a wearable sensor for ECG recording and with CGM is lacking.

The aim of this study is to assess the relationship that exists between HRV parameters computed in 5-minutes intervals and glycemia values in the same 5-minutes intervals, in a population of subjects affected by type 1 diabetes mellitus while carrying out activities of daily living monitored with a wearable sensor for ECG recording and with a CGM system for glycemia measurements.

1 Anatomy and physiology of the cardiovascular system

The cardiovascular system ensures blood flow to all organs of the body through the heart, which acts as a muscle pump, and the vessels, which form a blood distribution network and then return it to the heart. The cardiovascular system has one main subdivision: a pulmonary circulation, responsible for transporting blood to the lungs for the exchange of gases (oxygen O_2 and carbon dioxide CO_2) and used to bring it back to the heart, and a systemic circulation, which supplies the blood to every organ of the body (Figure 1.1). The right side of the heart supplies blood to the pulmonary circulation; it receives the blood that has circulated in the body, where it has released O_2 and nutrients and has picked up CO_2 and waste products. This oxygen-poor blood is pumped from the right side of the heart into the pulmonary trunk, a large caliber artery, which divides into the right and left pulmonary arteries that carry blood to the pulmonary alveoli where CO_2 is released and O_2 is picked up. Then, the oxygen-rich blood returns through the pulmonary veins to the left side of the heart where the systemic circulation originates. In the systemic circulation blood is pushed from the left side of the heart into the aorta, a large caliber artery. The aorta follows an inverted U-shaped course, the aortic arch, and then moves downwards behind the heart. Arteries that supply the head, neck and upper limbs originate from the aortic arch. The aorta then crosses the thoracic and abdominal cavities and branches into smaller arteries that reach the organs and then the lower limbs. The systemic blood, after having circulated throughout the body, is deprived of O_2 and returns to the right side of the heart through two large veins: the superior vena cava, which collects blood from the upper part of the body, and the inferior vena cava, which collects the blood from regions below the diaphragm. [1]

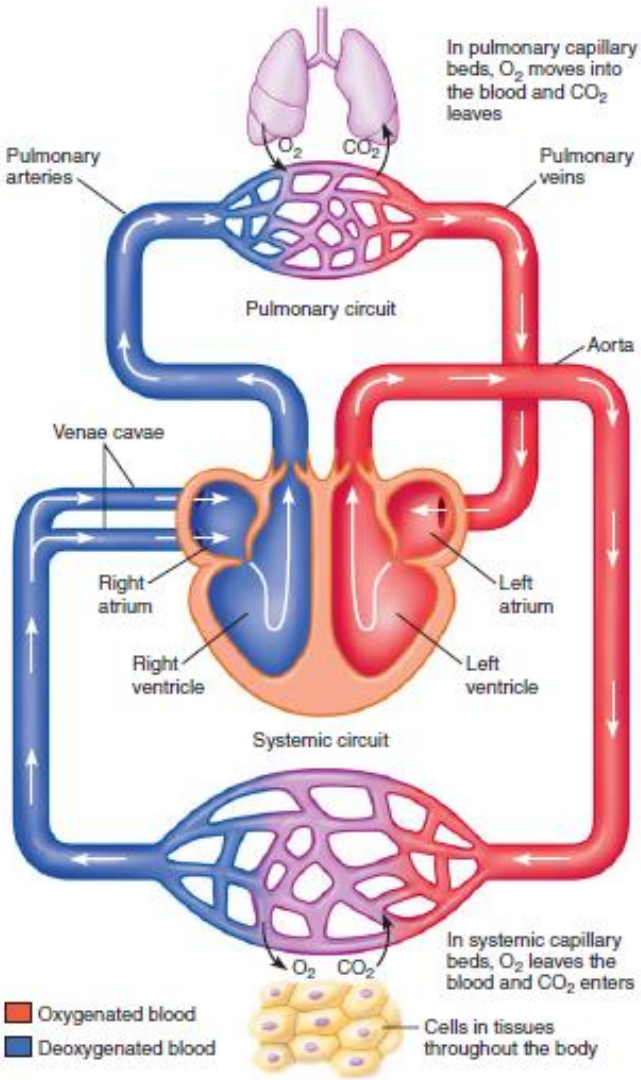

Figure 1.1 – The pulmonary and systemic circuits. [2]

1.1 The heart

The heart (Figure 1.2) is an organ located inside the thoracic cavity, in the mediastinum, the space between the two lungs and located behind the sternum. It works as a muscle pump that allows the flow of blood along the vascular tree. The major axis of the heart is bent to the left, in fact about two thirds of the heart occupy the left side of the median plane. The upper portion of the heart is wide and therefore it is called the base, while the lower portion of the heart narrows into a tip, the apex. An adult heart has a diameter of 9 cm at the base and the distance between the base and the apex is about 13 cm, the anteroposterior diameter at the level of the thickest point is about 6 cm, and its weight is about 300 g. The heart is enclosed in a sac, the pericardium, consisting of two sheets. The outer sheet, called the parietal pericardium, is provided with a superficial fibrous layer consisting of dense and irregular connective tissue in contact with a thin and deeper serous layer, called the epicardium or visceral pericardium, that lines the surface of the heart. Between the parietal and visceral sheets there is a space, called the pericardial cavity, which contains 5 to 30 ml of pericardial fluid that allows the heart to beat with minimal friction, isolates it from the other thoracic organs, and allows its chambers to expand by opposing to excessive expansion. The heart wall consists of three layers: the epicardium, the endocardium that lines the inside of the heart chambers, and the myocardium between these two layers and made up of heart muscle. The muscle tissue that makes up the myocardium coils around the heart so that when the ventricles contract, they perform a twisting and squeezing motion. The heart is also made up of a structure of collagen and elastic fibers called the fibrous skeleton and it is concentrated more at the level of the wall between the heart chambers, at the level of the fibrous rings around the valves, and in the laminae that connect these rings. The fibrous skeleton provides structural support to the heart by keeping the valves open and preventing them from overstretching as blood flows through them. The fibrous skeleton, not being a conductor of electricity, isolates the atria from the ventricles so that the atria cannot directly stimulate the ventricles. The heart is divided into four chambers; the two upper chambers are the left and right atria which collect blood returning to the heart through the large veins. The two lower chambers are the left and right ventricles which pump blood into the arteries. The boundaries of the four chambers are delimited by three sulci (grooves). The coronary (atrioventricular) sulcus separates the atria above from the ventricles below. The other two sulci extend from the coronary sulcus

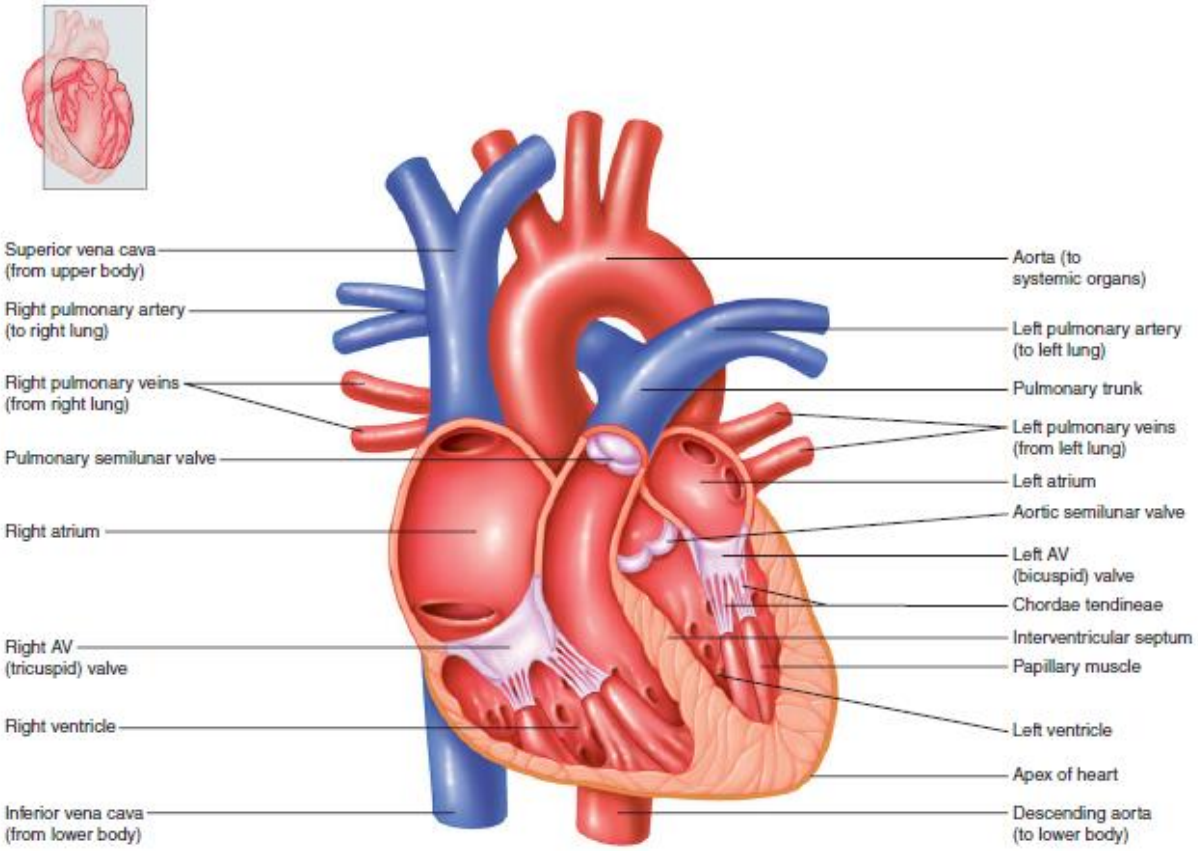

Figure 1.2 – A section of the heart showing the atria, ventricles, atrioventricular valves, and connections to major blood vessels. [2]

to the apex, one on the anterior face of the heart and it is called the anterior interventricular sulcus and one on the posterior face called the posterior interventricular sulcus. These sulci subtend an internal wall, the interventricular septum, which divides the right from the left ventricle. The atria have the function of pumping blood inside the ventricles and are separated from each other by a wall called the interatrial septum. To ensure unidirectional flow of blood, the heart is provided with valves (Figure 1.3). Each valve is made up of two or three fibrous sheets of tissue called cusps or flaps and are lined with endocardium. The atrioventricular (AV) valves regulate the passage of blood between the atria and ventricles. The right AV or tricuspid valve has three cusps while the left AV or bicuspid or mitral valve has only two. The chordae tendineae connect the valve cusps to the papillary muscles located on the floor of the ventricle. The papillary muscles prevent the AV valves from overturning or protruding inside the atria when the ventricles contract. The semilunar valves regulate the flow of blood from the ventricles to the large arteries. The pulmonary valve controls the orifice between the right

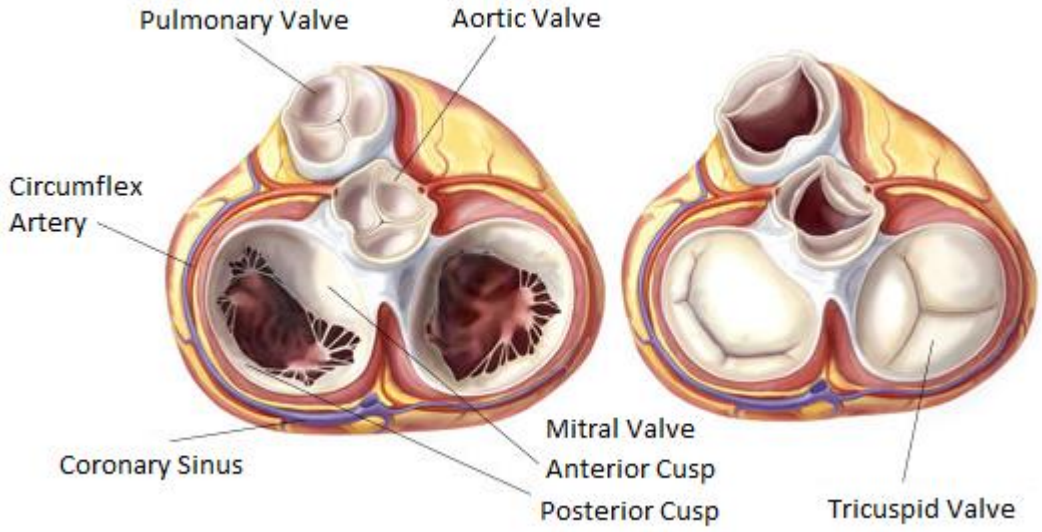

Figure 1.3 –The four heart valves. On the left we observe the open atrioventricular valves and the closed semilunar valves. On the right we observe the closed atrioventricular valves and the open semilunar valves.

ventricle and the pulmonary trunk while the aortic valve controls the orifice between the left ventricle and aorta. The semilunar valves are provided with three cusps but have no chordae tendineae. The opening and closing movement of the valves is not regulated by a muscular impulse of its own; the cusps are opened and closed by pressure changes that occur as the heart chambers contract and release. The blood from the right and left sides of the heart is kept totally separate. Since the heart is an organ subjected to a high workload, it beats on average 75 times per minute from the beginning to the end of an individual's life, it needs an abundant supply of nutrients and O_2. To meet the metabolic needs of the myocardium, it has its own set of arteries and capillaries that supplies it and delivers blood to each muscle cell. Coronary circulation starts from the aorta from which the right coronary artery and the left coronary artery originate and divide into smaller and smaller vessels, giving rise to a dense network of capillaries. [1]

1.2 The cardiac conduction system

The heart is mainly a muscle and the cells that make it up are the cardiocytes, short, stubby, and branched cells 50 to 100 micrometers long. Through these branches each cardiocyte contacts many others, thus forming an atrial network that envelops the atria and a ventricular network that envelops the ventricles. A cardiocyte has only one nucleus and the sarcoplasmic reticulum is less developed than in skeletal muscle and the T-tubules are much larger than those in skeletal muscle. Cardiocytes are joined at their ends by connecting systems called intercalated discs that also contain gap junctions that allow ions to flow from the cytoplasm of one cardiocyte into the cytoplasm of the next. The heartbeat is termed as myogenic since the signal is originated within the heart itself; the heart has its own pacemaker and electrical system. The heart muscle is almost entirely dependent on aerobic respiration to produce ATP. It is rich in myoglobin, a short-term source of oxygen and glycogen, which allows you to store energy. The heartbeat is coordinated by a cardiac conduction system consisting of an internal pacemaker and conduction pathways that branch into the myocardium. The conduction system generates and conducts rhythmic electrical signals in the following order (Figure 1.4):

1. The sinoatrial (SA) node, a portion of modified cardiocytes located in the right atrium just below the epicardium near the vena cava, is the pacemaker that starts each heartbeat and determines the heart rate (HR).
2. The signals from the SA node spread through the atria.
3. The AV node, located near the right AV valve at the lower end of the interatrial septum, transmits the stimulation to the ventricles while the fibrous skeleton acts as an insulator preventing the stimuli from reaching the ventricles by other routes.
4. The AV bundle or bundle of His represents the route through which electrical signals propagate as they leave the AV node. The bundle of His forks into the right and left branches which enter the intraventricular septum and descend to the apex.
5. The Purkinje fibers arise from the lower end of the branches of the bundle of His and fold upwards to spread inside the ventricular myocardium. They distribute the electrical excitation to the cardiocytes of the ventricles.

Although the heart has its own pacemaker, it receives sympathetic and parasympathetic innervation that changes the heart rhythm and the strength of contraction. Sympathetic stimulation increases HR and force of contraction and dilates coronary arteries to

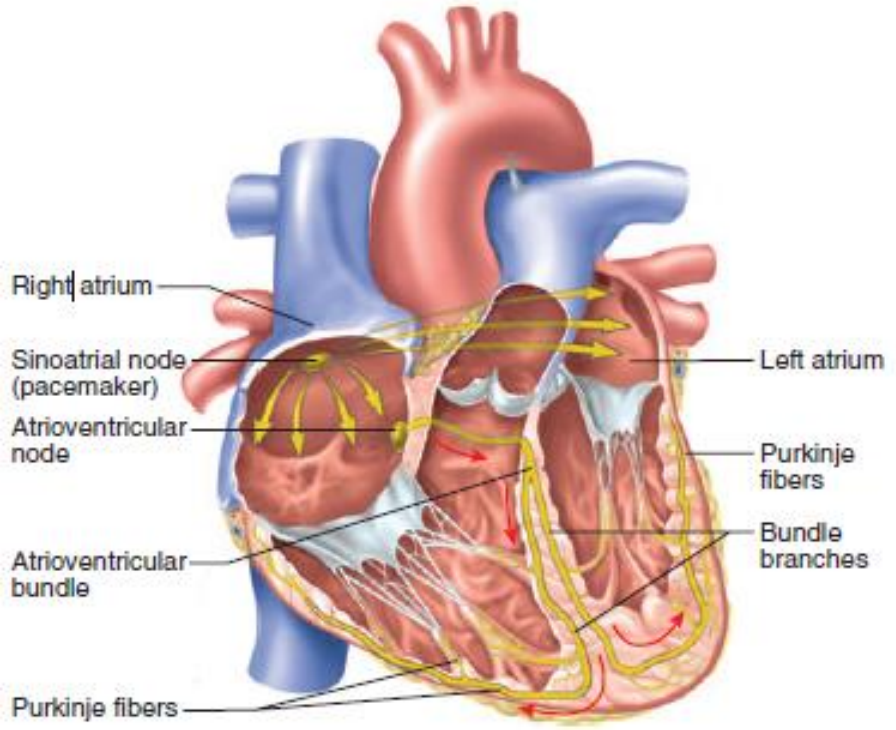

Figure 1.4 –The Cardiac Conduction System. Electrical signals travel along the pathway indicated by the yellow and red arrows. [3]

increase blood flow to the myocardium; parasympathetic stimulation can slow the HR by up to 20 beats per minute (bpm). The normal heartbeat triggered by the SA node is called the sinus rhythm, and at rest it has values of around 70-80 bpm. Any region other than the SA node that produces an impulse is called an ectopic focus. If the SA node is damaged, an ectopic focus can take over the heart rhythm producing an abnormal rhythm. Any abnormal heart rhythm is called an arrhythmia. The SA node discharge excites the atrial cardiocytes and stimulates the two atria to contract almost simultaneously. The signal travels at a speed of 1 m/s through the atrial myocardium and reaches the AV node. In the AV node the signal slows down to the speed of 0.05 m/s since the cardiocytes at this level are thicker and because they have fewer gap junctions through which the signal is transmitted. This delay is necessary to give the ventricles time to fill with blood before contracting. The signals travel through the bundle of His and the Purkinje fibers at a speed of 4 m/s, the ventricular myocardium depolarizes causing the almost unitary contraction of the ventricles. The signals reach the papillary muscles before the rest of the myocardium, they contract by straining the chordae tendineae an instant before the ventricular contraction pushes the blood against the AV valves. Ventricular systole starts from

the apex of the heart, which is the first region to be stimulated, and then progresses upwards pushing the blood through the semilunar valves. [1]

1.3 Electrical activity in pacemaker cells and in cardiac contractile cells

A cardiac contractile cell fires an action potential when it is depolarized to a threshold by an electrical current, a stimulus that comes from the near cells that are firing an action potential and that propagates through gap junctions. The pacemaker cells are different from the cardiac contractile cells because the pacemaker can fire action potentials without an external stimulus since it doesn't have a steady resting potential. Electrical signals are caused by changes in plasma membrane ion permeability, caused by opening and closing of ion channels. In cardiac muscle cells, the most important permeability changes involve sodium (Na^+), potassium (K^+), and calcium (Ca^{2+}) ions; the intracellular fluid of cardiac muscle cells is reach in K^+ but poor in Na^+ and Ca^{2+} with respect to extracellular fluid. The equilibrium potential for K^+, Na^+, and Ca^{2+} are respectively E_K = -94 mV, E_{Na} = +60 mV, and E_{Ca} = +130 mV. Hence, increased Na^+ permeability (P_{Na}) or Ca^{2+} permeability (P_{Ca}) makes the membrane potential more positive, while increased K^+ permeability (P_K) makes it more negative.

- Electrical activity in a pacemaker cell (Figure 1.5). In pacemaker cells, in the early stage of the pacemaker potential, the slow depolarization is due to the closing of K^+ channels and opening of the funny channels. The K^+ channels open during repolarization of the action potential and close when the membrane returns in the polarized state. Funny channels open after the cell repolarizes and allow Na^+ and K^+ ions to cross the plasma membrane. During the early stages of the potential the K^+ channels closes and funny channels open, decreasing the K^+ flow out of the cell and increasing the Na^+ flow into the cell, leading to the initial depolarization. The funny channels closes when the membrane potential reaches -55mV. The initial depolarization triggers the opening of voltage-gated Ca^{2+} channels called T-type channels; the T stands for "transient". The opening of the T-type channels increases P_{Ca} which depolarizes the cell even more; the T-type channels inactivate after a short time but the depolarization to threshold triggers

the opening of voltage-gated Ca^{2+} channels called L-type channels; the L stands for "long-lasting". This result in a big increment in P_{Ca} and the rapid depolarization. The depolarization triggers the opening of K^+ channels and a rise in P_K; this results in the repolarization of the membrane and the decrease in potential remove the stimulus for Ca^{2+} channel opening; consequently Ca^{2+} channel start to close, decreasing P_{Ca} and the flow of Ca^{2+} into the cell. The decrease in P_{Ca} together with the increase of P_K repolarize the membrane and terminate the action potential. [2]

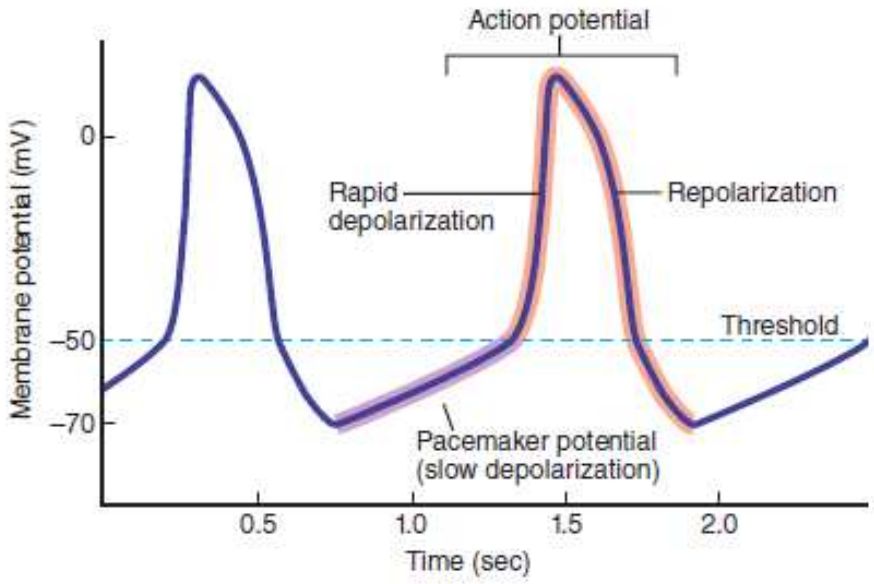

Figure 1.5 – Electrical activity in a pacemaker cell. [2]

- Electrical activity in a cardiac contractile cell (Figure 1.6). The action potential travels from the pacemaker to the other cells of the heart through the gap-junctions. The action potential of the cardiac contractile cells differs from the action potential of the pacemaker cells; cardiac contractile cells have a stable resting potential and have a longer-lasting action potential with a characteristic shape that can be divided into 5 phases, from phase 0 to phase 4.
    - Phase 0: depolarization of the membrane causes the opening of voltage-gated Na^+ channels, increasing P_{Na} and the flow of Na^+ into the cell. In consequence, the membrane potential becomes more positive, and this triggers the opening of still more Na^+ channels. The result is a rapid increase in the membrane potential with peaks between +30 and +40 mV.

- Phase 1: the Na^+ channels start to become inactivated, so P_{Na} is reduced and the flow of Na^+ into the cell is decreased; hence, the membrane potential becomes more negative. However, the membrane potential decreases slightly because the membrane depolarization, starting in phase 0, triggers in phase 1 the closing of voltage-gated K^+ channels called inward rectifier channels (decreases the flow of K^+ out of the cell) and the opening of L-type Ca^{2+} channels (increases the flow of Ca^{2+} into the cell) which act to depolarize the membrane.
- Phase 2: it is called the plateau phase. The K^+ channels that were closed during the phase 1 remain closed, and most of the Ca^{2+} channels opened in phase 1 remain open. These events maintain the membrane potential in the depolarized state.
- Phase 3: in response to the depolarization, a second population of K^+ channels, called delayed rectifier channels, opens. P_K increases and increases the flow of K^+ out of the cell, so the membrane potential becomes more negative. The fall of the membrane potential removes the stimulus that maintained the inward rectifier channels closed in phase 2, so these K^+ channels open and P_K increases even more. Furthermore, the fall of the membrane potential removes the stimulus that maintained the Ca^{2+} channels open in phase 2, so these Ca^{2+} channels close and P_{Ca} decreases, and it is reduced the flow of Ca^{2+} into the cell. The increase of P_K and the decrease of P_{Ca} repolarizes the membrane terminating the action potential.
- Phase 4: it is the resting phase, P_K, P_{Na} and P_{Ca} are at their resting values, but being P_K greater than P_{Na} and P_{Ca} the membrane potential is -90 mV, near the equilibrium potential of the K^+. [2]

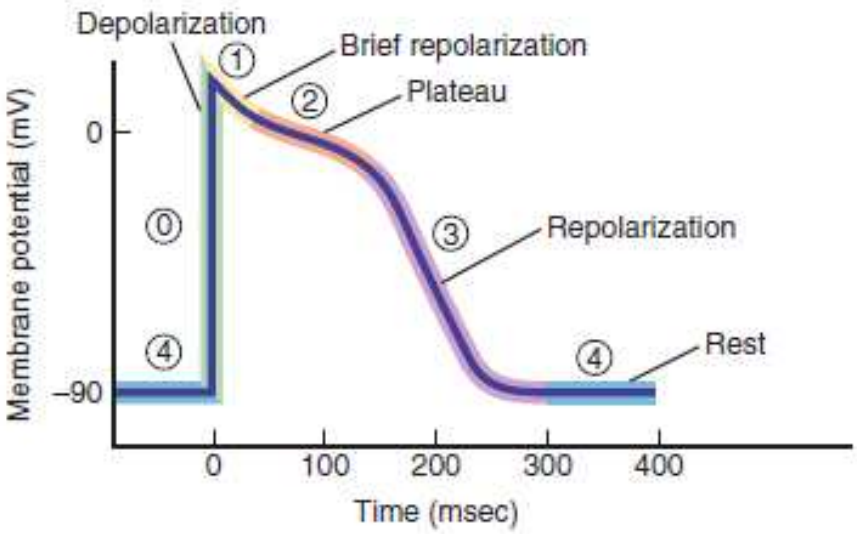

Figure 1.6 – Electrical activity in a cardiac contractile cell. [2]

1.4 Phases of the cardiac cycle

The cardiac cycle (Figure 1.7) is the period between the start of one heartbeat and the next. It consists of a complete series of contraction and relaxation of all four heart chambers regulated by the electrical events of the heart. All cardiac cycle events are completed in less than a second.

1. Ventricular filling. In diastole the ventricles expand, and their pressure becomes lower than that of the atria. Because of this, the AV valves open and blood flows into the ventricles, causing ventricular pressure to rise and atrial pressure to decrease. The right atrium contracts just before the left as it is the first to receive the signal from the SA node. At the end of the ventricular filling each ventricle contains an end-diastolic volume (EDV) of approximately 130 ml of blood and only 40 ml of this represents the contribution of the atrial systole.
2. Isovolumetric contraction. The atria repolarize, release, and remain in diastole for the remainder of the cardiac cycle. The ventricles depolarize and begin to contract. The pressure in the ventricles increases and reverses the pressure gradient between atria and ventricles. The AV valves close when ventricular blood exerts pressure against the cusps. This phase is called isovolumetric since, even if the ventricles contract, they do not yet expel the blood and therefore there is no change in their volume. In fact, since

the pressure in the aorta is 80 millimeters of mercury (mmHg) and in the pulmonary trunk is 10 mmHg, they are even greater than the pressure in the respective ventricles and therefore oppose the opening of the semilunar valves.

3. Ventricular ejection. When ventricular pressure exceeds arterial pressure, the semilunar valves are opened and blood is expelled. In the left ventricle the pressure reaches a peak of 120 mmHg while in the right ventricle the pressure reached is 25 mmHg. The ventricles do not expel all their blood. When the heart is at rest each ventricle contains an EDV of 130 ml; the amount expelled is about 70 ml and it is called stroke volume (SV); the amount of blood remaining is about 60 ml and is called the end-systolic volume (ESV).

$$EDV - SV = ESV \quad (1)$$

4. Isovolumetric relaxation. It is the early ventricular diastole that occurs when the ventricles begin to expand. Several hypotheses have been made about how they expand. The first hypothesis is that the blood flows inside the ventricles inflating them. The second hypothesis is that the contraction of the ventricles deforms the fibrous skeleton which subsequently comes back. This elastic return and expansion could cause a rapid decrease in pressure and leads to aspiration of blood inside the ventricles. At the beginning of ventricular diastole, blood flows briefly from the aorta and pulmonary trunk back to the semilunar valves, however this flow quickly fills the cusps and closes them. This phase is called isovolumetric because the semilunar valves are closed, the AV valves are not yet open, and the ventricles therefore do not receive blood. When the AV valves open ventricular filling starts again.

The pressure in the right ventricle is one fifth of the pressure in the left ventricle but both ventricles eject the same amount of blood. This is due to the low blood pressure in the pulmonary trunk, so the right ventricle does not need to generate high blood pressure to overcome it. It is imperative that both ventricles eject the same amount of blood. If the right ventricle pumped more blood into the lungs than the left ventricle could handle on return, the blood would accumulate in the lungs resulting in pulmonary hypertension and pulmonary edema. If the left ventricle expelled more blood than the right could handle on return, the blood would accumulate in the systemic circuit and lead to hypertension and edema. [1]

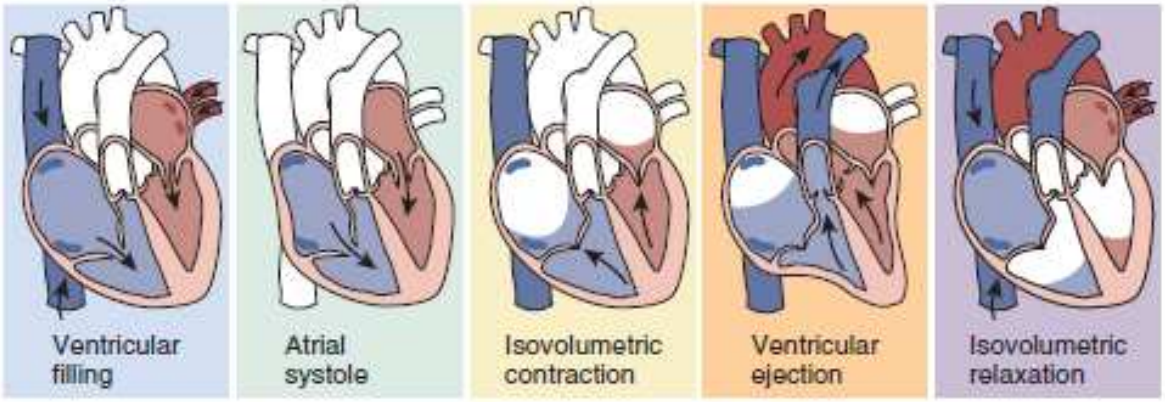

Figure 1.7 – Events that make up the cardiac cycle.

1.5 Neural regulation of the heart rate

The amount of blood pumped by the heart each minute is referred to as cardiac output (CO). HR is in beats/minute and the stroke volume (SV) is in ml/beat:

$$CO = HR \times SV \quad (2)$$

The total blood volume of the body (4-6 liters) passes through the heart every minute. It is deduced that cardiac output can be varied either by changing the HR or by changing the SV. The HR is regulated by the autonomic nervous system that modulate the activity of the SA node. Stroke volume is regulated by myocardial performance, which depends on the cardiocytes contractility, and by the hemodynamic loads of the heart. Modifications of the HR involve a reciprocal action of the two parts of the autonomic nervous system. The HR increases with a combined increase of sympathetic activity and decrease in parasympathetic activity; the HR decreases with a combined decrease of sympathetic activity and increase in parasympathetic activity. In a heathy and resting subject, the parasympathetic tone is usually predominant. [4]

- Parasympathetic pathways: the cardiac parasympathetic fibers have origin in the medulla oblongata, in the dorsal motor nucleus of the vagus nerve or in the nucleus ambiguus. The centrifugal vagal fibers pass through the neck and synapse with postganglionic vagal cells located on the surface of the epicardium or in the heart's walls. The vagus nerve has a right branch and a left branch. The right part of the vagus innervates predominantly the SA node and when this nerve is stimulated it slows down

the SA node firing and can even stop the firing. The left part of the vagus mainly inhibits the AV conduction leading to the AV block. However, the distribution of the left and right fibers of the vagus is almost overlapping so that the left vagal stimulation depresses also the SA node and the right vagal stimulation inhibits the AV conduction. Both SA and AV nodes are reach in acetylcholinesterase, an enzyme that rapidly hydrolyzes the neurotransmitter acetylcholine (ACh). Being the Ach rapidly destroyed, the effects of the vagal nerve stimulation decay quickly. Furthermore, the effects of the vagal stimulation on SA and AV nodes have a short latency (from 50 to 100 ms) because the released Ach activates some Ach-regulated potassium channels (K_{ACh}) in the cardiocytes. The rapid decay and the short latency of the effects of the vagal nerve stimulation allow them to exert a beat-by-beat control on SA and AV node activity [4]. The increased parasympathetic activity decreases the frequency of action potential in the SA node with the following mechanism (Figure 1.8): parasympathetic neurons release ACh which binds to muscarinic cholinergic receptors on the cells of the SA node, leading to an increase in the opening of K^+ channels and to the suppression of the opening of funny channels and T-type Ca^{2+} channels. This results in a decrease of the slope of the depolarization and a hyperpolarization of the membrane potential so the threshold for the next action potential is reached more slowly. This mechanism explains why the frequency of the action potential is decreased, leading to a decrease of the HR and of the cardiac output. Moreover, the increase of parasympathetic activity leads to a decrement in the speed of conduction of the action potentials, lengthening the time required by the action potential to reach the ventricles. This results in the increase of the duration of the systole. [2]

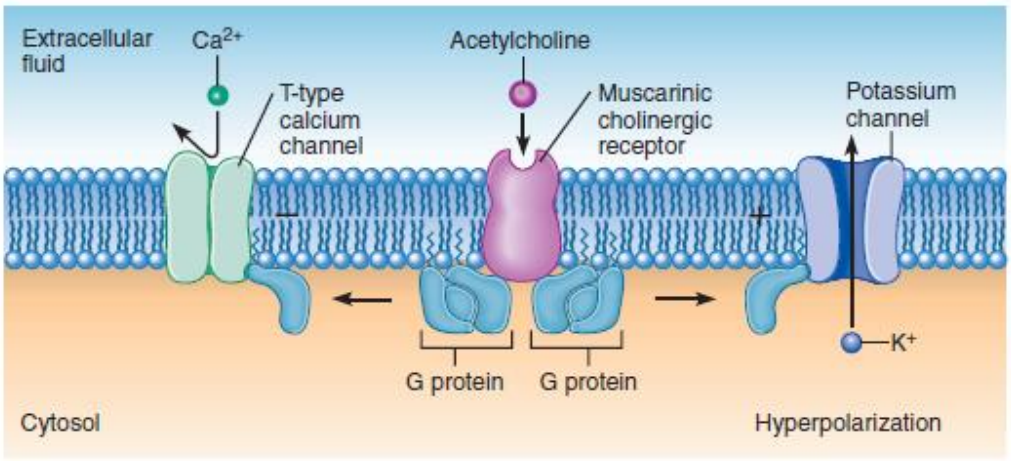

Figure 1.8 – The effects of the parasympathetic nervous system on the SA node.

- Sympathetic pathways: the cardiac sympathetic fibers have origin in the intermediolateral columns of the upper six thoracic segments and the lower two cervical segments of the spinal cord. These fibers exit from the spinal column passing through the white communicating branches and enter in the paravertebral chains of ganglia. The preganglionic fibers synapse with the postganglionic fibers in the stellate or middle cervical ganglia. Postganglionic sympathetic and preganglionic parasympathetic fibers join in the mediastinum forming a plexus of efferent nerves to the heart. The cardiac postganglionic sympathetic fibers of the plexus approach to the heart's base and then distribute to the chambers and penetrate the myocardium. Contrary to vagal activity, the effects of the sympathetic stimulation decay gradually after the end of the stimulation, and the increase of the HR due to sympathetic stimulation reaches the steady state more slowly than do the inhibitory effects of the parasympathetic stimulation. The slow onset of the cardiac response to sympathetic stimulation is due to the slow release of norepinephrine from the sympathetic nerve terminals and to the slow second messenger that mediates the cardiac effects of the released norepinephrine. Therefore, the sympathetic activity regulates the HR and the AV conduction more slowly than parasympathetic activity does; so while the parasympathetic activity exerts a control beat-by-beat, the sympathetic activity doesn't [4]. The increased sympathetic activity increases the frequency of the action potential in the SA node through the following mechanism (Figure 1.9): sympathetic neurons release norepinephrine which binds to β_1 adrenergic receptors on the cells of the SA node, and

this leads to the activation of the cAMP second messenger. The cAMP increases the opening of the funny channels and of T-type calcium channels. This results in an increase in the slope of the depolarization and a decrease in the level of repolarization, so the threshold for the next action potential is reached more rapidly. This mechanism explains why the frequency of the action potential is increased, leading to an increase in the HR and an increase in cardiac output. Moreover, the increase of the sympathetic activity leads to an increment in the speed of conduction of the action potentials, shortening the time required by the action potential to reach the ventricles. The result is that the ventricular contraction starts sooner after atrial contraction and proceeds more rapidly, decreasing the systole's duration. [2]

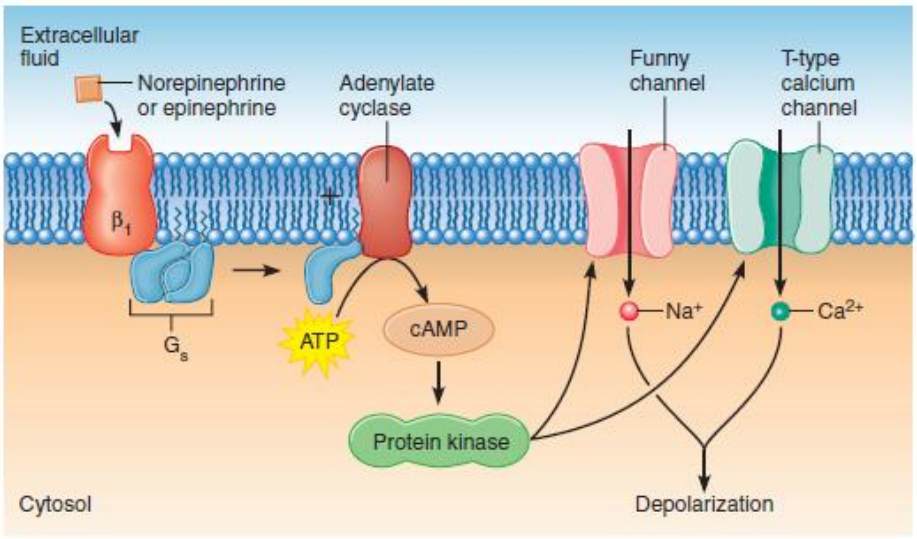

Figure 1.9 – The effects of the sympathetic nervous system on the SA node.

2 The electrocardiogram

The electrocardiogram (ECG) is a diagnostic tool used in clinical practice, especially useful for diagnosis of rhythm disturbances and changes in electrical conduction.

The heart's electrical signal, which originates from the SA node and spreads throughout the heart, is a flow of electrical currents. Since the thorax is a conductor, the electrical charges pass through it, generating an electric field on it. The equipotential lines of the electric field emerge on the thoracic surface, therefore placing two electrodes on two field lines with different potential will detect a potential difference. This potential difference varies as the depolarization and repolarization of cardiac fibers proceeds over time and its recording as a function of time is called an ECG. The detected potential differences depend on the position occupied by the electrodes. The shape of the equipotential lines generated by the cardiac electric field is the same as that generated by a dipole (Figure 2.1) consisting of two electric charges of opposite sign. The electrical activity of the heart can be thought to originate from a dipole which is called the equivalent electrical dipole of the heart. The effect of a certain number of charges, randomly distributed in a region of space, on a point P at a much greater distance than that existing between them, is the same as if they were concentrated in their charge center. For this reason, it is possible to represent all the positive charges of the heart with a single positive charge placed in a certain point inside the heart and all the negative charges with a single negative charge placed in another point. The dipole is characterized by an intensity which is a scalar quantity, equal to the dipole moment μ, and by a direction which is the axis of the dipole; the dipole can therefore be represented with a vector which is the cardiac vector H. Vector H is an expression of the instantaneous sum of the electrical activities of the heart. The speed of propagation of the electrical signal in the two branches of the bundle of His is different, the left ventricle contracts with a delay of 0.01 s with respect to the right ventricle. Depolarization proceeds from the inner surface of the ventricle wall to the outer surface. This means that the cardiac vector H, which represents the cardiac potential, varies over time in intensity and direction.

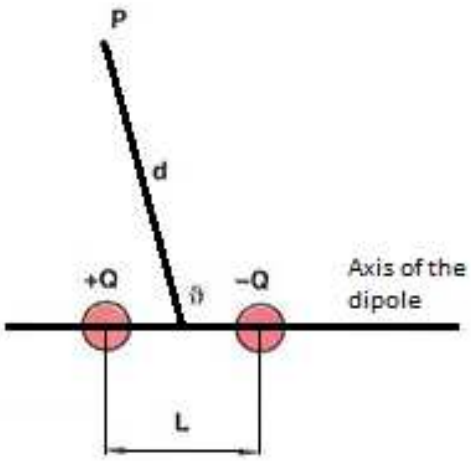

Figure 2.1 - Schematic diagram of an electric dipole: μ dipole moment, Q dipole charge, d distance of the point P from the center of the dipole, ϑ angle between the axis of the dipole and the line connecting point P with the midpoint of L.

2.1 The position of the electrodes

For the detection of cardiac potentials, at least two electrodes placed on the surface of the body in non-equipotential places are required. Since the recordable potential differences depend on where the electrodes are placed, it is essential to standardize the positions where to place them in order to make ECGs performed at different times and places comparable. The Dutch physiologist Einthoven schematized the human body as a conductor containing the source of electrical activity at its center. He placed the electrodes at the vertices of an equilateral triangle in the center of which he imagined the heart to be and indicated with A the right arm, with B the left arm and with C the base of the sternum. Since the arms and legs behave like open circuits in which no current induced by the dipole flows, the potential assumed by the left arm is approximate to the potential of point B, the same is true for the right arm and for the legs (which have potential approximable to the potential assumed by point C). The three electrodes constitute the nodes of a mesh to which we can apply the first Kirchhoff principle which allows us to deduce the value of a lead knowing the other two potential differences. The triangle in Figure 2.2 is called Einthoven's triangle and points A, B, C are identified respectively as RA (right arm), LA (left arm), LL (left leg). The straight lines joining RA with LA, RA with LL, and LA with LL identify three directions that can be represented respectively with three versors a_1, a_2, a_3, which constitute an equilateral triangle. The

projections of the vector H on the directions a_1, a_2, a_3 identify scalar quantities V_1, V_2, V_3 according to the relation:

$$V_i = H \cdot a_i \qquad i = 1, 2, 3 \tag{3}$$

They are therefore the scalar product between the cardiac vector H and the versors a_i. Particularly:

- the potential difference measured between RA and LA, that is $V_{LA} - V_{RA} = V_I$ takes the name of lead I;

- the potential difference measured between RA and LL, that is $V_{LL} - V_{RA} = V_{II}$ takes the name of lead II;

- the potential difference measured between LA and LL, that is $V_{LL} - V_{LA} = V_{III}$ takes the name of lead III.

With this definition and bearing in mind that Einthoven's triangle is a closed mesh, we have that $V_{III}+V_I=V_{II}$, that is, at every instant the second lead is equal to the sum of the first and of the third and this regardless of the position of the electrodes. In fact, in diagnostic ECG recording, the anatomical site of RA is the right wrist, of LA the left wrist, and of LL the left ankle. At the center of Einthoven's triangle we observe the vector H, whose components on the directions identified by the three leads provide the scalar value of V_I, V_{II}, V_{III}. The scalar value is what the

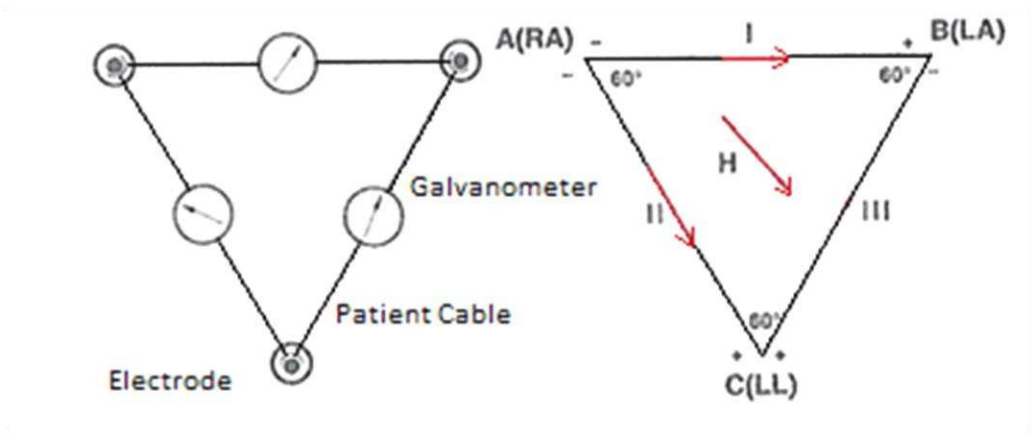

Figure 2.2 – Einthoven's triangle: standard bipolar leads. On the left we observe the connecting circuit, on the right we observe the projection of the cardiac vector H.

instrument measures and therefore the recording of two of the three leads allows to reconstruct the vector H, having assumed a decomposition according to the directions defined by the Einthoven triangle. The three leads are also called bipolar because 2 of the 3 electrodes available are required to register them. Another way to perform an ECG uses unipolar leads, the instrument detects the potential at an anatomical site with respect to a reference. In 1944 Wilson proposed to evaluate the displacement of the cardiac vector H during the cycle on a horizontal plane, using unipolar leads and as a reference an electric center W called the Wilson Central Terminal. The Wilson Central Terminal is formed by connecting each electrode constituting the three main leads to a common node by means of a resistance of the same value R. By adding an exploring electrode E, the potential differences with respect to W were evaluated in certain sites called P_1, P_2, P_3, P_4, P_5, P_6 occupying the anatomical position shown in Figure 2.3. These potential differences are called precordial leads and are indicated with V_1, V_2, V_3, V_4, V_5, V_6. These leads reflect the activity of the heart as a whole and allow a more complete picture of the position of the H vector and its anomalies to be obtained.

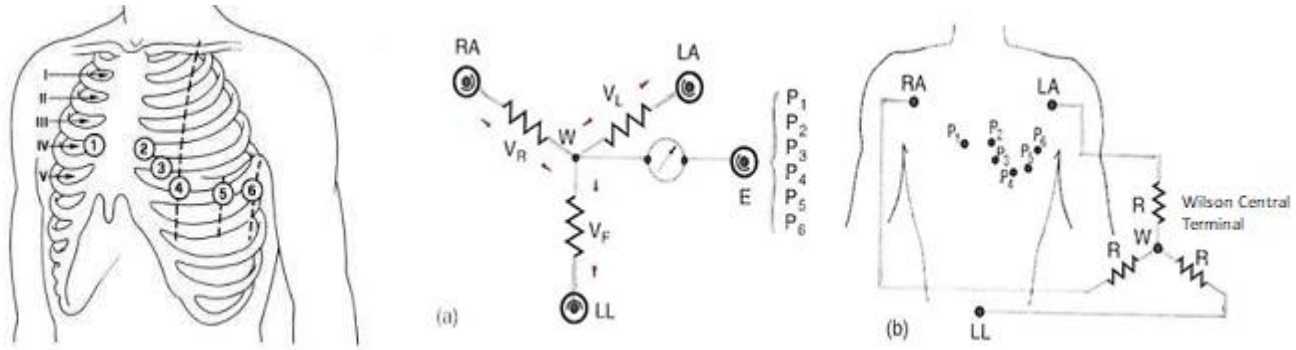

Figure 2.3 - The precordial leads. Arrangement of electrodes and circuit configuration.

Augmented leads are also needed for this purpose. They are three and use RA, LA, LL as the signal sampling point; they are unipolar as they are determined with respect to the reference potential V_W. The three augmented leads called aV_R, aV_L, aV_F, are obtained by eliminating the resistor that in the Wilson circuit is connected respectively to the right arm, left arm, left ankle and replacing it with the instrument to measure the potential difference. These leads are called augmented (Figure 2.4) because, again referring to the Wilson circuit, the potential difference detectable between the reference pole W' and the corresponding limb is increased by 50% due to the elimination of the resistor R. The augmented leads are useful because they allow to

make a projection of the cardiac vector on the sides of an equilateral triangle rotated by 30° counterclockwise with respect to that of Einthoven and therefore allow a new view without moving the electrodes (Figure 2.5).

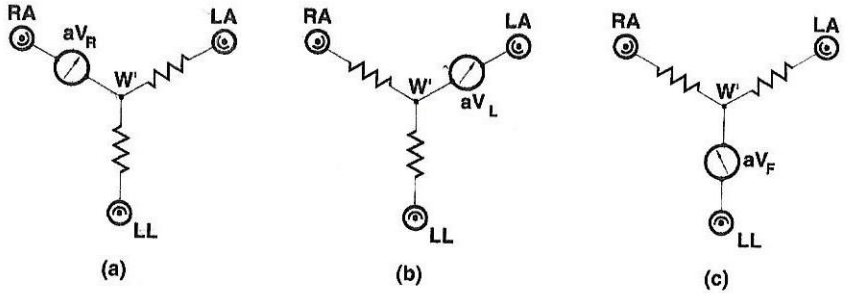

Figure 2.4 - Circuits related to the recording of the cardiac potential through the augmented leads.

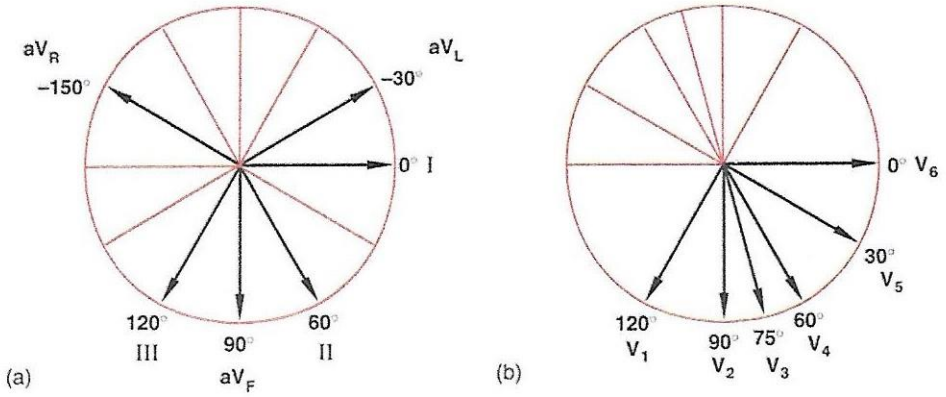

Figure 2.5 - Projections of the components of the vector H in the frontal (a) and transverse (b) plane.

The following relationships are valid:

$$aVR = -\tfrac{1}{2} \cdot (I + II) \qquad (4)$$

$$aVL = \tfrac{1}{2} \cdot (I - III) \qquad (5)$$

$$aVF = \tfrac{1}{2} \cdot (II + III) \qquad (6)$$

Where I, II, III are the standard leads and aV_R, aV_L, aV_F are the augmented leads. [5]

2.2 The electrocardiographic tracing

An electrocardiograph allows to record the trace resulting from cardiac activity on graph paper with two speeds: 25 mm/s or 50 mm/s. An electrocardiograph allows to obtain separately the 12 leads of the H vector: the 3 standard leads, the 3 augmented leads and the 6 precordial leads. Let's study an electrocardiogram (figure 2.6) obtained in the second lead which is the one that provides the widest QRS signal. The first deflection, called the P wave, corresponds to the depolarization of the atria. Subsequent waves, called QRS, result from the depolarization of the ventricles; the Q wave is an initial negative wave; the R wave is a positive deflection that follows the Q wave; the S wave is a negative deflection that follows the R wave. The T wave represents the repolarization of the ventricles and is sometimes followed by the U wave whose meaning is still unclear today [5]. The repolarization of the atria occurs during the PR interval or the QRS complex, for this reason its identification is difficult. The PQ interval is a measure of the time from the onset of atrial activation to the onset of ventricular activation and a prolongation of this interval is associated with disturbances in AV conduction. During the ST interval the ventricles are depolarized, therefore the ST segment normally lies on the isoelectric line. The QT interval, also called “period of electrical systole of the ventricles” has a duration that varies inversely with the HR. [4]

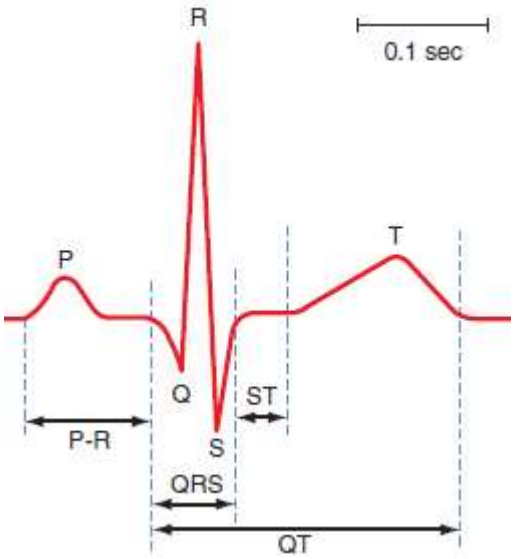

Figure 2.6 – Deflections and intervals of a second lead ECG. [4]

3 Heart-rate variability

Heart rate variability (HRV) (Figure3.1) is the measure of the time variation in R–R intervals during sinus arrhythmia, denoted as “N–N” intervals; it represents the influence of the autonomic nervous system on the SA node. Although the SA node has an intrinsic firing rate that can be studied blocking the action of the autonomic nervous system, physiologic sinus arrhythmia reflects parasympathetic and sympathetic activity. Hence, HRV is a non-invasive marker of the activity of the autonomic nervous system. Large HRV is an indicator of a healthy heart, the oscillations of a healthy heart are complex and constantly changing allowing the cardiovascular system to rapidly adjust to sudden physical and psychological challenges reaching the homeostasis, while depressed HRV is associated with many diseases, with myocardial infarction and heart failure. While the activity of the parasympathetic nervous system increases HRV, the activity of the sympathetic nervous system decreases it; therefore, HRV is typically higher when the heart beats slowly and lower when the heart starts beating faster. HRV can be measured in both time and frequency domains with a series of estimates, also called parameters. The time domain estimates of HRV that are more commonly used are:

- The standard deviation of all NN intervals (SDNN). It is a quantification of the total HRV and reflets both sympathetic and parasympathetic activity on the heart.
- The standard deviation of all average NN intervals (SDANN) for all 5-minute segments within the defined time period. It reflects the circadian rhythm.
- The average of the standard deviation of all NN intervals (ASDNN) for all 5-minute segments within the defined time period. It reflects both sympathetic and parasympathetic activity on the heart.
- The root mean square of successive NN interval differences (RMSSD). It reflects the parasympathetic activity on the heart.
- The HR, the number of beats per minute.
- The HRV triangular index (TRI) [6], that is a geometric measure based on 24 h ECG recordings which calculates the integral of the density of the RR interval histogram divided by its height. Usually, to represent this metric a 5-min epoch is used. [7]
- The triangular interpolation of the NN interval histogram (TINN) is the baseline width of a histogram displaying NN intervals. [7]

- Approximate Entropy (ApEn). It is a measure of the regularity and complexity of a time series; large ApEn values indicate low predictability of fluctuations in successive RR intervals while small ApEn values indicate that the signal is regular and predictable. [7]
- The number of successive NN intervals whose difference is > 50ms (NN50).
- The ratio between NN50 and all NN in the defined time period (pNN50). It reflects the parasympathetic activity on the heart. [7]
- The measure of the standard deviation of instantaneous RR interval variability derived from the RR Poincarè plot (SD1).
- The measure of the continuous long-term RR interval variability derived from the RR Poincarè plot (SD2). [8]
- The ratio between SD1 and SD2 (SD1/SD2). It measures the unpredictability of the RR time series. [7] [8]

HRV frequency domain features are calculated from the RR tachograms using the fast Fourier transformation [9]; In the frequency domain, HRV can be classified into distinct bandwidths of high (0.15–0.40 Hz), low (0.04–0.15 Hz), very low (0.0033–0.04 Hz), and ultralow (<0.0033 Hz) frequencies. Vagal activity modulates HRV in all frequency bands.

- The high frequency (HF) component of HRV at 0.15–0.40 Hz mainly reflects the parasympathetic activity and the respiratory sinus variation from vagal activity that is predominant in health state.
- Low frequency (LF) activity at 0.04–0.15 Hz reflects sympathetic activity that increases in disease states such as heart failure.
- Very low frequency (VLF) activity at 0.0033–0.04 Hz reflects parasympathetic activity but may also indicate activation of the renin-angiotensin-aldosterone system.
- Ultralow frequency (ULF) activity, below 0.0033 Hz, is of uncertain physiologic meaning. [6]

The HRV frequency domain features comprise the absolute values of the power of each band and the ratio between the power bands [9]. There is a close analogy between the time domain indices of HRV and frequency bandwidths. There is an 80% correlation for SDNN with total spectral power, SDANN with ULF power, ASDNN with VLF power. Therefore, time and frequency domain methods measure the same physiologic phenomena. Depressed HRV is associated with many pathological states; HRV may be attenuated after a myocardial infarction due to autonomic denervation or distortion of sensory nerve endings from altered myocardial

geometry. HRV is also reduced in heart failure patients and in patients with diabetic neuropathy; the HRV magnitude reduction is a predictor of ventricular fibrillation. [6]

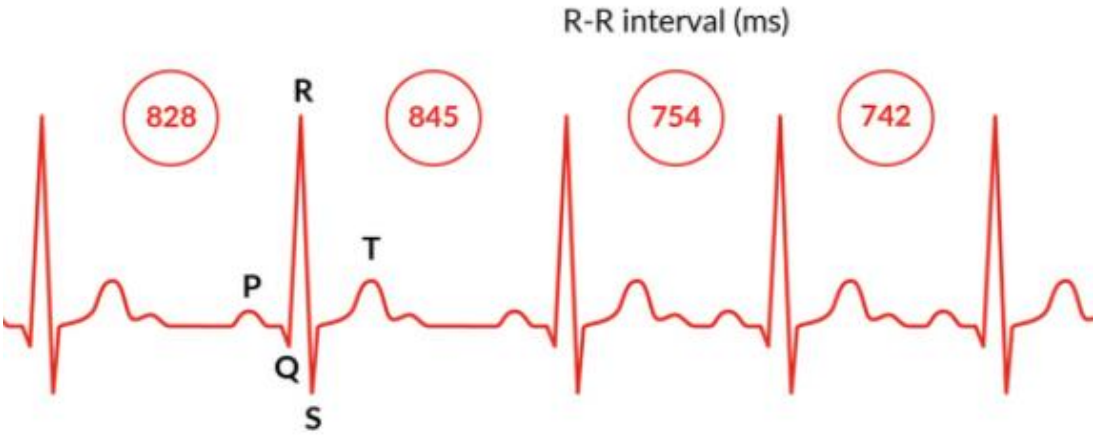

Figure 3.1 - Variation of the temporal distance between R peaks.

3.1 Data acquisition and signal processing

For HRV analysis are required raw ECG data; usually it is sufficient to digitize the data at a frequency of 250 Hz. The first step in computing HRV is to annotate beats from long term ECG recordings and to classify the beats into “normal sinus beats” (designated “N”), supraventricular beats (designated “S”), and ventricular beats (designated “V”). As HRV processes beat-to-beat intervals (RR), ectopic beats, that introduce big and sudden changes in the beat-to-beat interval relative to sinus beats, can have a significant effect on HRV calculations; ectopic beats can be managed in different ways depending on whether time or frequency domain methods are used. Ectopic beats can be managed by simple deletion when using time domain techniques, but this is not possible when using frequency domain techniques because the deletion will affect the results of the fast Fourier transformation. One possible solution is to replace intervals generated by ectopic beats with RR intervals generated by averaging the preceding and succeeding RR intervals or to use higher order interpolation. Then ECG data must be resampled at a constant frequency to calculate HRV in the frequency domain. ECG contains QRS complexes at variable rather that fixed intervals of time and because each measurement of the RR interval occurs at the time of a QRS complex, this results in a series of data points (RR intervals) that are sampled unevenly over time. To apply the fast Fourier transformation to this data, additional time points must be added to the original beat

series to make uniform the sampling times and then we must interpolate appropriate RR intervals for these points. Any frequency faster than the highest HR found in the recorded ECG can be used as the resampling frequency, although usually it is used a frequency notably greater than the HR, such as 4 Hz. [6]

4 The body's metabolism

Eating is a biological necessity because food is the sole source of energy and the raw material from which the human body is made. For the human being it is not possible to eat continuously to maintain a constant energy supply to meet the body's needs; for this reason, the body must store nutrients during meals (carbohydrates, proteins, and lipids) and then break down the store of nutrients between one meal and the next. During the meal, the large molecules of food are broken down into smaller molecules by the gastrointestinal tract in a process called digestion. The small molecules are then absorbed into the bloodstream and distributed to the tissues of the body and taken up by cells; carbohydrates are transported in the blood as glucose, proteins are transported as amino acids, and lipids are transported in lipoproteins. These biomolecules can be broken down into smaller molecules in a process that releases energy that is used for cellular processes such as contraction and transport; they can be used as substrates for the synthesis of other molecules, for tissue growth and repair; furthermore, biomolecules in excess of those required for energy and synthesis of other molecules are transformed in energy storage molecules such as glycogen and triglyceride. [2]

4.1 Energy metabolism

To maintain the homeostasis, the energy in input to the human body must be equal to the sum of the energy utilization (energy used to perform work within cells) plus the energy output (energy in the form of heat released).

$$\text{Energy input} = \text{energy utilization} + \text{energy output} \quad (7)$$

$$\text{Energy input} = \text{work performed} + \text{heat released} \quad (8)$$

The energy input into the body comes from the absorbed nutrients; when a nutrient molecule is oxidized in the body, a certain quantity of energy, the energy content of the molecule, is released. The energy content of the molecules of the three nutrient classes is: 4 kilocalories per gram of carbohydrate, 4 kilocalories per gram of protein, 9 kilocalories per gram of fat. The human body is not in energy balance at any instant of time because feeding is intermittent; for the 3-4 hours after the meal the nutrients are absorbed, and the body is in the absorptive state.

During this state the rate of energy input exceeds the energy output, so the body is in positive energy balance; glucose is used as the primary energy source for the cells while fats, amino acids, and excess glucose are absorbed by the liver, muscle, and fat cells and converted in energy storage molecules.

- Skeletal muscle cells take up glucose and amino acids from the blood to satisfy their own needs and to convert glucose to glycogen for storage.
- The liver converts nutrient molecules into storage of energy that can subsequently be mobilized to guarantee energy to most cells of the body. The liver converts glucose to glycogen that then is stored in the liver. It also converts glucose to fatty acids and fatty acids to triglycerides which are transported to adipose tissue for storage. The liver also takes up amino acids to synthesize proteins and converts amino acids to keto acids that are used to synthesize fatty acids and so triglycerides, then transported to adipose tissue.
- Adipocytes store energy in the form of triglycerides; excess absorbed glucose enters in the adipocytes and is converted to triglycerides.

The postabsorptive state is the time between meals, when nutrients are not being absorbed; during this state the rate of energy output exceeds the rate of energy input, so energy stores are used to provide energy to the cells. Since glucose is the sole energy source for cells in the central nervous system, in the postabsorptive state the other cells of the body use other energy sources such as fatty acids, sparing glucose for the central nervous system. In order to guarantee enough plasma glucose, the body synthesizes new glucose from amino acids, from glycerol and from other breakdown products of catabolism; this process is called gluconeogenesis.

- In skeletal muscle cell, glucose formed from glycogen through glycogenolysis can be used for energy only within that muscle cell. Skeletal muscle cells can catabolize proteins to amino acids which are then transported to the liver.
- The liver is the primary source of plasma glucose during the postabsorptive state, in fact it converts glycogen stores into glucose through glycogenolysis, and then glucose is transported into the bloodstream and can be used by the cells of the body. The liver is the primary site of gluconeogenesis and here occurs ketogenesis, the conversion of fatty acids into ketone bodies which are then released into the bloodstream and can be used

as a source of energy by the cells of the central nervous system during prolonged fasting.

- Adipocytes catabolize stored triglycerides into glycerol and free fatty acids. Glycerol travels in the bloodstream reaching the liver and it is catabolized by glycolysis. Free fatty acids are released into the bloodstream and then can be used as energy source by body cells.

The human body is able to switch between absorptive and postabsorptive states thanks to the action of hormones that regulate the body metabolism. There are two hormones that play a fundamental role in the regulation of the whole-body metabolism, insulin and glucagon, both secreted by a gland, the pancreas. [2]

4.2 Regulation of absorptive and postabsorptive metabolism

The pancreas (Figure 4.1) is an extramural gland located retroperitoneally, inferior and dorsal to the stomach. It is 15 cm long and 2.5 cm thick and most of it is an exocrine digestive gland but, scattered through the exocrine tissue, there are clusters of endocrine cells called pancreatic islets or islets of Langerhans. There are 1 to 2 million islets, but they represent only about 2% of the pancreatic tissue. The islets secrete hormones and paracrine products, the most important of which are insulin, glucagon, and somatostatin. [3]

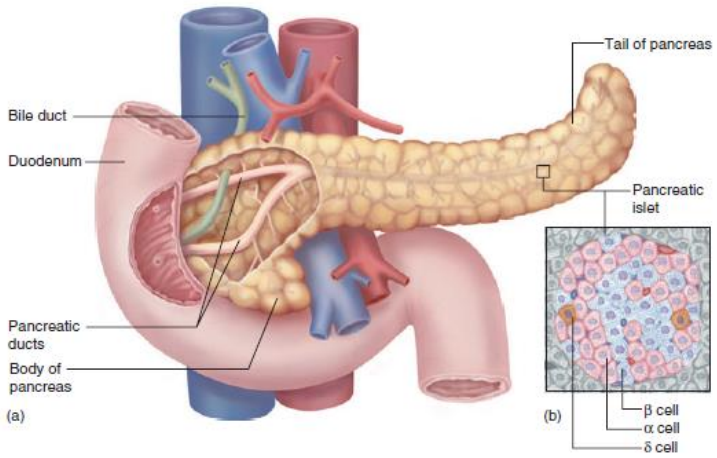

Figure 4.1 - Macroscopic anatomy of the pancreas (a); cells from a pancreatic islet shown with histological staining (b); [3]

4.2.1 The role of Insulin

Insulin is a peptide hormone secreted by β cells located in the islets of Langerhans; insulin promotes the synthesis of energy storage molecules and the processes characteristic of the absorptive state. During the absorptive period insulin secretion increases causing plasma insulin levels to increase, while during the postabsorptive state insulin secretion decreases causing plasma insulin levels to decrease which turn off the absorptive state processes. During the absorptive period glucose is transported into the bloodstream from the gastrointestinal tract; this increase of blood glucose concentration stimulates the production of insulin by β cells (Figure 4.2). Glucose enters β cells by facilitated diffusion through GLUT2 transporters, it is catabolized in a process that generates ATP, and ATP closes K^+ channels in the β cell membrane. With less K^+ moving out of the cell, the β cell becomes depolarized, and this leads to the opening of Ca^{2+} channels. Ca^{2+} enters in the cell and triggers insulin exocytosis.

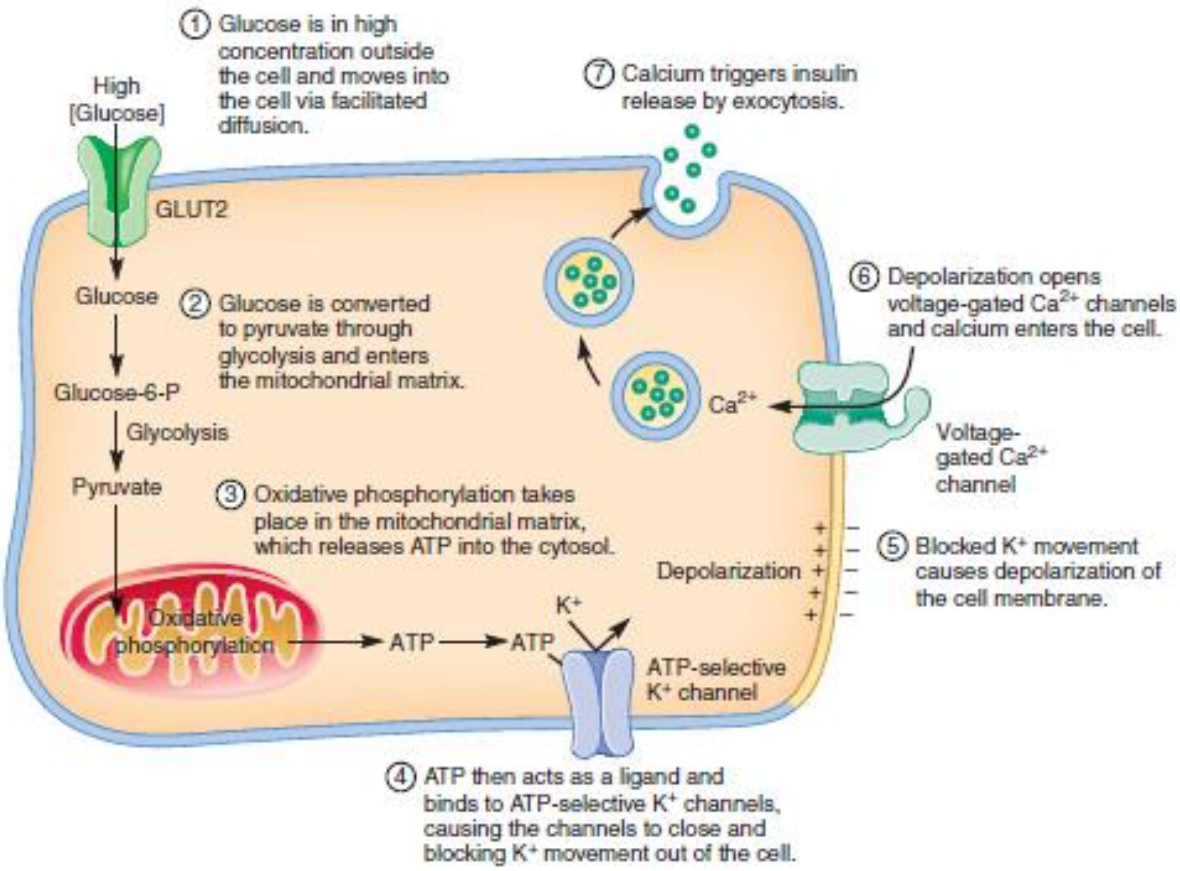

Figure 4.2 – Glucose stimulated insulin secretion.

During the postabsorptive period the levels of plasma glucose decrease and consequently insulin secretion is reduced. Insulin production is also stimulated by the increment of plasma amino acid concentration with a process similar to the glucose stimulated insulin secretion. Insulin secretion is also stimulated by parasympathetic nervous system activity, by glucose-dependent insulinotropic peptide (GIP), and glucagon-like polypeptide 1 (GLP-1), two hormones secreted by cells in the wall of the small intestine. Parasympathetic nervous system activity and GIP and GLP-1 secretion increase with the presence of food in the gastrointestinal tract and because feeding occurs before the nutrients absorption, this is a feedforward mechanism to prepare the body to the absorptive state by triggering insulin secretion before the increment of plasma glucose levels. Instead, the sympathetic nervous system activity and circulating epinephrine inhibits insulin secretion. Insulin promotes energy storage by stimulating the synthesis of fatty acids and triglycerides in the liver and adipose tissue, of glycogen in liver and skeletal muscles, and of proteins in most tissues. At the same time insulin counteracts the catabolism of energy stores by inhibiting the breakdown of proteins, triglycerides, and glycogen, and by suppressing gluconeogenesis by the liver. Briefly, insulin promotes the characteristic events of the absorptive state and suppresses the characteristic events of the postabsorptive state. Insulin stimulates the uptake of amino acids from plasma into cell with insulin-sensitive active transporters, facilitating protein synthesis. Insulin stimulates the uptake of glucose from plasma into the cell by increasing the number of glucose transport proteins in cell plasma membranes. Thirteen different glucose transporters are coded in the human genome, called GLUT1 through GLUT13, but only one of these transporters, GLUT4, is sensitive to insulin. GLUT4 is a facilitated diffusion transporter for glucose; skeletal muscle and adipose tissue cells have pools of GLUT4 transporters that are stored in vesicles in the cytoplasm, and insulin triggers the insertion of these transporters into the plasma membrane. Exercise also triggers expression of GLUT4 on the plasma membrane of skeletal muscle cells and adipocytes. Insulin influences the transport of nutrients across the membranes of all body cells but not in liver cells and central nervous system cells. This is very important because when insulin levels are low during the postabsorptive state, the uptake of glucose by most cells is decreased, sparing the glucose for use by cells of the central nervous system, where glucose transport is not influenced by insulin. Moreover, during the postabsorptive state, the liver produces glucose that is transported into the blood. [2]

4.2.2 The role of Glucagon

Glucagon is a peptide hormone secreted by α cells of islets of Langerhans. Insulin and glucagon are antagonists, their actions oppose each other because insulin promotes processes of the absorptive state and glucagon promotes processes of the postabsorptive state; glucagon secretion decreases during the absorptive state and increases during the postabsorptive state. Most of the signals that stimulate the secretion of glucagon are the same signals that inhibit the secretion of insulin, an example is the decrement of blood glucose that stimulates glucagon secretion and inhibits insulin secretion. Sympathetic nervous activity and epinephrine stimulates glucagon secretion and inhibits insulin secretion. Furthermore, insulin inhibits the secretion of glucagon from α cells and glucagon inhibits the secretion of insulin from β cells, so while plasma glucagon levels rise plasma insulin levels decrease and vice versa. In the liver, glucagon promotes glycogenolysis and gluconeogenesis increasing blood glucose levels, promotes ketone synthesis and breakdown of proteins, and inhibits glycogen and protein synthesis. In adipose tissue, glucagon promotes lipolysis and inhibits triglyceride synthesis. So, glucagon promotes all the characteristic events of the postabsorptive state, promoting mobilization of the stores of energy and the synthesis of glucose and ketone bodies. Insulin and glucagon together control plasma glucose concentration through negative feedback, an increase in plasma glucose concentration increases insulin secretion and decreases glucagon secretion, reducing plasma glucose. Similarly, a decrease in plasma glucose concentration decreases insulin secretion and increases glucagon secretion, increasing plasma glucose. In this way plasma glucose levels are tightly regulated, and this is of fundamental importance because deviations too far from normal plasma glucose level can have serious adverse effects on health. [2]

4.2.3 Effects of sympathetic nervous system and epinephrine on metabolism

Sympathetic nervous system and epinephrine stimulate glucagon secretion and suppress insulin secretion, so promote the metabolic adjustments characteristic of postabsorptive state; in fact, the postabsorptive period is characterized by reduced plasma glucose levels, which act on α and β pancreatic cells increasing glucagon secretion and decreasing insulin secretion. Moreover, a decrease in plasma glucose levels acts on glucose receptors in the central nervous

system to raise the level of activity in sympathetic neurons, which triggers a rise in epinephrine secretion by the adrenal medulla. The raise in plasma epinephrine acts on the liver to raise glycogenolysis and gluconeogenesis, on skeletal muscle to raise glycogenolysis, and on adipose tissue to raise lipolysis. Similar actions are promoted by sympathetic neural input to the liver and adipose tissue, while skeletal muscle cells do not receive input from sympathetic neurons. Under normal conditions the control of sympathetic nervous system on metabolism is minor than the control exercised by insulin and glucagon. The importance of the sympathetic influence on metabolism becomes evident in the body's reaction to stress, a term that indicates any condition that poses a serious challenge to the body's ability to maintain homeostasis. The word stress includes both physical conditions, such as dehydration, hemorrhage, infection, exposure to extremes temperature, trauma, or severe exercise, and psychological states, such as pain, fear, or anxiety. Activation of the sympathetic nervous system by stress triggers the fight-or-flight responses which encloses accelerated HR, generalized vasoconstriction, dilation of respiratory airways. It also increases plasma glucose levels due to increased gluconeogenesis and glycogenolysis in the liver, and it increases plasma levels of fatty acids and glycerol due to increased lipolysis in adipocytes. These actions provide fuel to cells by helping to prepare the body for the strenuous physical activity of the fight-or-flight response, for tissue repair, and to fight infection. [2]

5 Diabetes

The term glycemia refers to the blood glucose concentration. In healthy subjects, who have a regular life and a correct diet, generally the blood sugar values remain between 60 and 130 mg/dl during the day. When fasting, glycemia values can vary from 70 to 110 mg/dl; between 100 and 125 mg/dl it is a condition of impaired fasting glycemia (IFG), a condition that should encourage the patient to pay more attention to his lifestyle. Glycemia values equal to or greater than 126 mg/dl are considered, according to the American Diabetes Association, probable symptoms of diabetes. Nowadays, two categories of diabetes mellitus (DM) can be distinguished: type 1, also called insulin-dependent or juvenile-onset DM; and type 2, also called insulin-independent or adult-onset DM. Type 1 DM is an autoimmune disease in which the immune system attacks the β cells of the pancreas, destroying them, and consequently causing a loss of insulin secretion from these cells that becomes insufficient to regulate blood glucose. In type 1 DM, the cause of the wrong immune response has genetic basis, but also environmental factors play a role, such as viral infections that may unmask a genetically predisposed form of type 1 DM. At approximately 7 years of age (when 80% or more of the beta cells are destroyed), symptoms begin to appear such as hyperglycemia and lethargy. Type 2 DM is associated with insulin resistance, a condition in which insulin target cells show a decreased response to insulin. Although the causes of insulin resistance are unknown, several factors predisposing individuals to this condition have been identified, such as genetics (more than in type 1 DM), sedentary lifestyle and obesity. Type 2 DM generally develops after age 45 but the age at time of diagnosis is decreasing and the number of children developing type 2 DM is increasing. Diabetes mellitus predisposes a person to hyperglycemia that may cause hypotension, headaches, fatigue, blurred vision, difficulty thinking, and mood changes. Severe hyperglycemia can lead to ketoacidosis, a dangerous metabolic acidosis that arises when cells use fats for energy instead of glucose. In fact, when hyperglycemia occurs in type 1 DM most cells of the body cannot use blood glucose without insulin that induce glucose transporters into the cells' plasma membranes; thus, the cells must use fats. Cells use fatty acids to produce ATP by β oxidation and oxidative phosphorylation, and the by-products of this β oxidation process travel to the liver, where they are converted to ketones, causing ketoacidosis. Also, hyperglycemia induces epinephrine release in response to hypotension (hyperglycemia

increases urine output causing hypotension because of the osmotic pull of excess filtered glucose on water). To restore blood volume and pressure to normal values the sympathetic nervous system is activated, and epinephrine is released promoting gluconeogenesis and glycogenolysis which mobilizes glucose for use as an energy source, thus increasing hyperglycemia. Patients with DM may suffer from hyperosmolar nonketotic coma when their glucose levels reach extremely high levels, between 600 and 2400 mg/dl. This extremely high glucose levels cause more glucose, and thus more water, to be lost in the urine, leading the person to dehydration. Severe dehydration leads to hypovolemia, which decreases blood flow to the tissues. If enough fluid is lost such that blood osmolarity increases to a level greater than 325 mOsm, the person goes into a coma. Also, coma can be caused by taking of too much insulin for the treatment of DM, and in this case it is called hypoglycemic coma; so hypoglycemic coma is a problem of mismanagement of DM. Indeed, hypoglycemia is defined as a blood glucose level less than 50 mg/dl and the symptoms associated with it are nausea, hunger, cold or wet skin, trembling, and tachycardia during mild stages, and if allowed to progress hypoglycemia causes blurred vision, confusion, dizziness, anxiety, lethargy, seizures, loss of consciousness and coma. DM can be controlled through diet, lifestyle changes, insulin administration and other medications. Maintaining normal glycemia levels prevents or slows the progression of advanced symptoms. DM affects blood vessels throughout the body, but the mechanism of vasculature pathology is different in type 1 DM and in type 2 DM. In type 1 DM hyperglycemia increases blood flow and pressure in the microcirculation, and this causes shear stress to the blood vessels damaging endothelial cells, scarring the microvasculature, and thickening the basement membrane. Scarring limits the ability of arterioles to dilate and induces rigidity, so tissues may be deprived of increased blood flow during times of need, leading to tissues damage. Type 2 DM decreases the vasodilatory responses of the microvasculature, and this phenomenon is probably due to a decreased production from endothelial cells of nitric oxide, a vasodilator. A lack of nitric oxide release will leave arterioles constricted, decreasing blood flow to tissues. Damage to the microvasculature contributes to several diabetic conditions such as retinopathy, nephropathy, neuropathy, and delayed wound healing. One of the most debilitating complications of DM is diabetic neuropathy that can result in pain, autonomic dysfunction, and even amputation. Diabetic neuropathy takes place in the peripheral nervous system, affecting afferent and efferent pathways of both the somatic and autonomic nervous systems. Hyperglycemia leads to nerve and glial cell damage by many

mechanisms including glycosylation, oxidative stress, and increased activity of the polyol pathway. Neuropathies associated with sensory afferents can cause paresthesia that is an abnormal sensation of the skin such as tingling, or numbness, and dysesthesia that is an unpleasant sensation produced by normally innocuous stimuli or pain. Loss of sensibility to the feet may contribute to diabetic foot, a person may be unaware of a sore on the foot, and if not correctly treated sore becomes infected, gangrene can set in, and amputation may be required. Neuropathy of somatic efferent pathways, that is motor neurons to skeletal muscles, can cause muscle weakness, and neuropathies of the autonomic nervous system can affect almost any organ in the body. Cardiac autonomic neuropathy may lead to cardiac infarction, arrhythmias, and cardiac arrest, and one symptom is the HRV decrement. Also, reflex control of autonomic functions can be damaged, and this reduce the body's ability to maintain homeostasis. [2]

5.1 Diabetes therapy and Continuous Glucose Monitoring

Glycemic self-monitoring is indispensable in type 1 DM and insulin-treated type 2 DM to calibrate therapy and to define the necessary insulin doses to prevent acute and late complications. Daily glycemic self-monitoring is an integral part of the therapeutic strategy since glycemic values can change over the course of the day and greater awareness of the patient can help in the constant monitoring of their condition. Glycemic self-monitoring is made easier by the availability of various types of glucometers, which adapt to the various needs of patients, for example there are glucometers that suggests the insulin bolus to administer during the meal [10].

Glucometers are devices for the rapid determination of glycemia on capillary blood obtained by pricking the tip of a finger. The drop of blood is placed on a test strip inserted into the reading instrument. The principle on which is based the measurement, in the most common glucometers, consists in the quantification of an enzymatic reaction, the oxidation of glucose, which is proportional to its concentration in the blood. The reaction occurs by placing a blood sample on a glucose-oxidase test strip. The measurement can be obtained with a reflectometric technique (color intensity determined by the chromogen that develops from the oxidation of glucose) or impedancemetric technique (electrical conductivity of the blood induced by the

electric current generated by the oxidation of glucose). Another method used for glycemia measurement is the Continuous Glucose Monitoring (CGM); CGM is a fairly recent technology that involves the continuous measurement of glucose levels in the interstitial fluid. Each CGM device consists of a sensor fixed to the skin and a visualization and recording system. Compared to traditional self-monitoring methods, CGM devices continuously detect glucose levels, thus offering the advantage of having many measurements available throughout the day, circa 300 measurements, and the possibility of evaluating glycemia variability in time. CGM systems are devices equipped with a detection system that, using an enzymatic reaction, measures the concentration of glucose in the subcutaneous interstitial fluid that surrounds the cells; they are associated with a conversion system that transforms the variations of glucose levels in digital electronic signals of intensity proportional to the concentration of glucose. The monitoring systems most used today use “minimally invasive” needle-cannula sensors. The needle sensor consists of a cannula, which is implanted under the skin, a few mm long, inside which there is a platinum electrode and a matrix containing the detection enzyme, glucose-oxidase. This enzyme, in presence of glucose and oxygen, catalyzes a reaction which leads to the production of an electron current proportional to the glucose levels. An algorithm transforms the potential difference into glucose concentrations, based on capillary blood glucose values taken as a reference at different times of the day [11]. However, most people who use blood glucose measurement systems, even if only minimally invasive, report a sense of discomfort or limitation in daily activities; for this reason, it would be a big step forward to develop a non-invasive sensor capable of measuring blood glucose reliably.

6 Glycemic variability

Chronic hyperglycemia is the primary cause of the development of DM related complications but also frequent or large glucose fluctuations, such as postprandial spikes and hypoglycemic events, contribute to complications development. The term glycemic variability (GV) refers to blood glucose oscillations that occur throughout the day, including hypoglycemic periods and postprandial spikes, as well as blood glucose fluctuations that occur at the same time on different days. Glycemia changes are the physiological consequences of carbohydrate intake and of the circadian rhythm of hormones involved in the glucose metabolism control. So, while a certain degree of GV is not negative and it is observed in people with normal glucose tolerance, an increased GV is observed in people with DM and with IFG. The occurrence of microvascular and macrovascular complications in DM is attributed to hyperglycemia and dysglycemia (peaks and nadirs) and the two primary mechanisms leading to vascular complications are excessive protein glycation end products and activation of oxidative stress. Several studies have shown that intermittent high blood glucose exposure, rather than constant exposure to high blood glucose, has cardiovascular deleterious effects. The mechanisms that are at the basis of the adverse cardiovascular effects of GV are mainly associated with oxidative stress. There is a significant association between GV and the increased incidence of hypoglycemia. Hypoglycemic events may induce the release of inflammatory cytokines leading to inflammation and may induce an increased platelet and neutrophil activation; hypoglycemia also leads to sympathoadrenal response that increases adrenaline secretion and may induce arrhythmias and increase the cardiac workload; the underlying endothelial dysfunction leading to reduced vasodilation may contribute to cardiovascular risk. GV is particularly important in type 1 DM, where the succession of hyperglycemia, normoglycemia, and hypoglycemia are linked to insulin deficiency, erratic absorption of exogenous insulin, incomplete suppression of hepatic glucose production and altered hormonal regulation. Studies performed using CGM showed a significant fluctuation in blood glucose values of children with type 1 DM, even if the glycated hemoglobin (HbA1c) values, used as an assessment test for glycemic control in people with diabetes, are excellent. These results indicate that GV may have a predictive value for the development of type 1 DM complications. Some studies also demonstrated that HbA1c is a poor predictor of hypoglycemic risk, whereas GV is a strong predictor of hypoglycemic

episodes. It is also shown a significant association of GV with retinopathy in patients with type 1 DM and type 2 DM [12]. A study performed on type 1 DM subjects suggests that GV plays an important role in the development of peripheral neuropathy and that the nervous system is particularly vulnerable to blood glucose fluctuations [13] [14]. Given the close relationship between GV, oxidative stress and DM complications, GV is becoming a focus for future treatments aimed at guarantee greater efficacy in the control of the metabolic alterations of DM and the prevention of the associated complications. Nevertheless, the definition of GV remains a challenge primarily due to the difficulty of measuring it because of the lack of consensus regarding the optimal approach for its measurement [14]. Researchers use CGM data to assess how glucose levels vary across the day and night for several days or weeks and to identify its health impact, so a series of indices for GV measurement have been proposed and they can be obtained from CGM data:

- Mean glucose level, the mean of glucose values.
- Standard Deviation (SD), an index of the dispersion of data around mean glucose level.
- Coefficient of Variation (CV), the ratio of the SD to the mean of glucose values in percentage.
- J-index, a composite metric based on mean and standard deviation of glucose values.
- Post-event area under the curve, mean of the blood glucose measurements in the 15 minutes occurring 1 hour or 2 hours after medication, meal, or physical exercise events.
- The Mean Amplitude of Glucose Excursion (MAGE), the mean of the daily glucose excursions that exceed the SD measured over the 24 hours period.
- Continuous Overall Net Glycemic Action (CONGA), SD of the differences between *n* hours apart measurements; the higher the CONGA value, the greater the glycemic excursion.
- Low Blood Glucose Index (LBGI) and High Blood Glucose Index (HBGI), the frequency and extent of low and high glucose measurements, respectively. Higher LBGI and HBGI values indicate respectively more frequent or more extreme hypoglycemia and hyperglycemia. In a non-diabetic and non-pregnant population hypoglycemia is defined as <3.3 mmol/l and hyperglycemia as ≥10mmol/l.
- Blood Glucose Risk Index (BGRI), LBGI + HBGI, an indicator of the risk of undergoing extreme glycemic values.

- Average Daily Risk Range (ADRR), average sum of the highest and lowest glucose values for each day.
- Area Under the Curve (AUC), it characterizes the overall glucose levels; it is calculated for each hour using the trapezoidal rule. The AUC average over the whole 24 hours period is returned as the average AUC.
- Time Above Range (TAR), percentage of time spent by the glucose trace above a certain range.
- Time Below Range (TBR), percentage of time spent by the glucose trace below a certain range.
- Time in Range (TIR), percentage of time spent by the glucose trace within the normal blood glucose range.
- Standardized Glycemic Variability Percentage (sGVP), length of the flattened glucose trace after being standardized, it reflects the degree of trace undulation due to peaks and valleys.
- Post-event time to peak, the number of minutes between the meal and the subsequent glucose peak value.
- Mean Absolute Deviation (MAD), represents the overall variability of glucose values and considers time points as a set of non-normally distributed values; it is a measure of dispersion.
- Fasting Proxy, measure of fasting glucose levels computed as the mean of the six lowest consecutive glucose values (with 5 minutes intervals) occurring before breakfast. [14] [15] [16]

7 State of the art on the relationship between heart-rate variability and glycemia and between heart-rate variability and glycemic variability.

7.1 State of the art on the relationship between heart-rate variability and glycemia

Some studies have been carried out in recent years in order to identify how glycemic events affect and modify HRV. One of these is the study of Nguyen et al. [17]; Nguyen et al. evaluate, in a hospital setting, the effects of hyperglycemia on HRV in 6 type 1 DM patients during night, acquiring ECG and blood glucose levels every 30 minutes. The time domain HRV parameters computed are mean RR interval, SDNN, RMSSD, and pNN50. Frequency domain parameters studied are the power of LF, HF, VLF, and the ratio between LF and HF components (LF/HF) that reflects the balance between sympathetic and parasympathetic activity. Pearson's correlation analyses are used to evaluate the strength of association between blood glucose levels and HRV variables in time and frequency domains and significance value (p-value) less than 0.05 is considered significant. SDNN, RMSSD, pNN50, LF power, and HF power result to be significantly decreased under hyperglycemic condition compared to non-hyperglycemic condition. Mean RR and LF/HF are also reduced but without achieving statistical significance. This result agrees with other studies that describe lower HRV in diabetic patients than in normal subjects [18] [19]. So, blood glucose levels are inversely and significantly correlated with SDNN, RMSSD, pNN50 and LF and HF powers, and SDNN is the most significant HRV parameter with a strong relation with hyperglycemia. Hence, in agreement with other studies, high blood glucose levels cause lower HRV in subjects with DM and SDNN, LF and HF power could be good markers to identify hyperglycemic events from HRV in type 1 DM [17]. Similar results are obtained in the study of Rothberg et al. [20] where 32 participants with DM and 31 without DM are studied. The study is

conducted in this way: fasting preceded a 10-minutes ECG which is followed by a finger prick blood glucose assessment; following this, a regular meal is consumed, and 30 minutes after ingestion a second 10-minutes ECG is obtained, and blood glucose assessment is repeated. LF power and HF power are found to be negatively associated with blood glucose levels in participants with DM, but contrary to the study of Nguyen et al. [17] LF/HF is positively correlated with glycemia [20]. Furthermore, Nguyen et al. [21] find that hypoglycemia increases HR, while hyperglycemia decreases HRV. It is also reported that hypoglycemia can alter the ECG pattern by prolonging the QT interval [21]. The association between HRV and glycemia is also studied by Singh et al. [19] in a large population of 1919 men and women using ambulatory ECG recordings and fasting plasma glucose measurements. HRV variables considered are SDNN, HF and LF power, and LF/HF. Fasting plasma glucose levels are used to classify subjects as normal (<110 mg/dl), as having IFG levels (110 to 125 mg/dl), and as having DM (≥126 mg/dl or receiving therapy). It results that SDNN, LF and HF power, and LF/HF are inversely related to plasma glucose levels ($p < 0.0001$). SDNN, LF and HF powers, and LF/HF are reduced in diabetic subjects and in subjects with IFG compared with those with normal fasting glucose. So HRV is inversely associated with glycemia and is reduced in diabetics as well as in subjects with IFG [19]. Some studies have focused the attention on the relationship between HRV and the ability of the body to manage glucose. One of these is the study of Vishinov et al. [8]. It is part of the Glyco project, a project which aims at detecting the blood glucose levels from the ECG. The study included 155 patients with instantaneous fasting blood glucose level measurements, and the aim of this study is to understand if HRV parameters describe the body's ability to control the fasting blood glucose level at the time of the measurement of HRV. ECG is measured by a single lead wearable sensor and the HRV parameters extracted are: SDNN, ASDNN, SDANN, NN50, pNN50, RMSSD, SD1, SD2, SD1/SD2. The research uses the Pearson's correlation and the Spearman's rank correlation. For the 5-minutes HRV it is found only a strong positive correlation of the fasting glucose with SD1/SD2 and a negative correlation of the fasting glucose with SDNN and with ASDNN. Therefore, this study concludes that 5-minutes HRV parameters can't indicate a strong linear correlation with the ability of the body to regulate blood glucose levels but can motivate further research [8]. Stein et al. [22] test the hypotheses that increased HR and decreased HRV are present in people with IFG not in the range of DM, and in people with metabolic syndrome independent of elevated fasting glucose levels. HR and HRV are found in 1267 people who have Holter monitoring; 536 of them have normal fasting glucose levels,

363 have mildly IFG, 182 have significantly IFG, and 178 have DM. HRV parameters studied are SDNN, SDANN, ASDNN, pNN50, and RMSSD. HRV parameters turned out to be more impaired in subjects with significantly IFG and with DM than in subjects with normal fasting glucose or mildly IFG. There were few differences in HRV parameters between subjects with normal fasting glucose and mildly IFG or between subjects with significantly IFG and with DM. In subjects with normal fasting glucose or mildly IFG having two or more components of metabolic syndrome is associated a greater decrease in HRV parameters compared with subjects having no or one components of metabolic syndrome. In subjects with significantly IFG or with DM, metabolic syndrome is associated with decreased HRV parameters compared with no metabolic syndrome. Increased HR and diminished HRV occur in mildly and significantly IFG. Decreased HRV is associated with metabolic syndrome, independent of fasting glucose levels. These results suggest that factors associated with mildly and significantly IFG and with the metabolic syndrome play a role in the decrement of HRV and so with the onset of cardiac autonomic neuropathy [22]. Similar results are obtained by Coopmans et al. [23], in fact, also in this study, subjects with IFG and with DM present HRV time and frequency domain parameters lower than in normal subjects. The amount of which HRV is lower in IFG compared with normal fasting glucose subjects is half of that in type 2 DM in both time and frequency domains. In addition, glucose levels result linearly associated with HRV, which suggests a graded decline in HRV with worsening glucose tolerance. These results suggest that cardiac autonomic neuropathy is already present in IFG subjects, and so before the development of DM. Hyperglycemia may cause cardiac autonomic neuropathy via increased oxidative stress, endothelial dysfunction, and the formation of advanced glycation end products, all of which may lead to neuronal damage and subsequent autonomic neuropathy. In addition, some studies suggest that autonomic neuropathy causes hyperglycemia via impaired insulin release by the pancreas, increased glucose production by the liver, and altered glucose uptake and insulin resistance in skeletal muscles. Thus, it is possible that exists a vicious cycle of hyperglycemia and autonomic neuropathy. [23]

7.2 State of the art on the relationship between heart-rate variability and glycemic variability

To date, in the literature, there are no studies on the relationship between HRV and GV carried out on subjects with type 1 DM in every-day life conditions and monitored simultaneously with wearable sensors and CGM. One of the few studies that takes into account GV and HRV at the same time is that of Lespagnol et al. [24] whose aim is to explore the impact of a 9-day cycling tour on HRV in a population of 20 amateur athletes with uncomplicated type 1 DM, with a focus on exercise induced glycemic excursions. Throughout the days of the tour subjects wore the CGM system Dexcom G4 Platinum to examine glycemic excursions and variability. They concomitantly wore the heart rate monitor Polar H7 to assess HRV at night and during time spent at different exercise intensities. HRV is analyzed during sleeping period between midnight and 4:00 am throughout the 9 days of the cycling tour. HRV time domain parameters analyzed are SDNN, pNN50, and RMSSD; HRV frequency domain parameters analyzed are HF and LF power. Glycemic excursions and variability are calculated from CGM recordings over several periods: from midnight to 4:00 am concomitant with the period of HRV analysis, the day before from the beginning of breakfast to 2 hours post dinner, over periods of 24 hours, and during the cycling periods excluding the lunch and during early and late recovery (2 hours and 6 hours after the cycling periods). Glycemic excursions studied are the percentage of time spent in the normal range (between 70 and 180 $mg \cdot dl^{-1}$), in level 1 hypoglycemia (between 54 and 69 $mg \cdot dl^{-1}$), in level 2 hypoglycemia (less than 54 $mg \cdot dl^{-1}$), in level 1 hyperglycemia (between 181 and 250 $mg \cdot dl^{-1}$), in level 2 hyperglycemia (between 251 and 300 $mg \cdot dl^{-1}$), and hyperglycemia more than 300 $mg \cdot dl^{-1}$. GV indices studied are CV, SD, MAGE, CONGA and ADRR. The results show that parasympathetic tone parameters such as HF power, pNN50, RMSSD, and sympathetic-vagal balance represented by LF/HF do not vary significantly with time throughout the tour and are not altered by the characteristics of the performed exercise; the results also show that global HRV, represented by SDNN, decreases with the number of kilometers traveled the day before. Furthermore, this study concluded that global HRV was not linked with glycemic excursions and a decrease in sympathetic-vagal balance and an increase in parasympathetic tone during the night were associated with longer time spent in level 1 hypoglycemia during the previous day and the 6 hours recovery period after exercise. A decrease in parasympathetic tone during the

night was associated with a longer time spent in a state of level 2 hyperglycemia during the same night, as well as with hyperglycemia more than 300 $mg \cdot dl^{-1}$ in the previous day [24]. In the study of Klimontov et al. [25] it is investigated the associations of frequency-domain HRV parameters with antecedents and contemporaries interstitial glucose fluctuation in women with type 2 DM at high cardiovascular risk. 67 women with type 2 DM, including 46 ones with cardiovascular autonomic neuropathy, underwent Holter recording and CGM at the same time. GV indices computed from CGM data include SD, CONGA, J-index, MAGE, mean absolute glucose, LBGI and HBGI. HRV parameters considered are LF and HF power computed on 5 minutes intervals in both fasting and postprandial conditions, and during the night in correspondence of CGM defined hypoglycemia. The study results show that the values of LF and HF power reduce after meals in type 2 DM women with normal autonomic function while patients with cardiovascular autonomic neuropathy demonstrate blunted postprandial LF and HF power reduction and diminished LF/HF during daytime hypoglycemia. Daytime LF and HF power values in fasting conditions correlate negatively with mean absolute glucose obtained from the previous night CGM, while fasting LF power correlates positively with nocturnal LBGI. Negative correlations between LF power during daytime hypoglycemia and nocturnal CONGA, J-index, HBGI and mean absolute glucose are also seen. The HBGI and CONGA measured during night are predictors of LF power during daytime hypoglycemia. [25]

8 Study of the relationship between heart-rate variability and glycemia

8.1 Materials and methods

8.1.1 The dataset

In the present study the dataset used is the one of Dubosson [26], the unique publicly accessible dataset offering ECG and glucose time series acquired both with wearable devices and in real-life conditions. This dataset was collected in the context of the D1NAMO project, a project which aim is to detect glycemic events through non-invasive ECG pattern analysis. The D1NAMO dataset is composed of 9 patients with type 1 DM recruited during a routine clinic visit at Hopital Riviera-Chablais in Vevey. The dataset contains the following data: ECG signals, breathing signals, accelerometer outputs, glucose measurements, food pictures and annotations by a dietitian. The acquisition of ECG, breathing, and accelerometers outputs was made using the Zephyr BioHarness 3.0 device. Information collected at patient enrollment are age, weight, height, and sex (Table 1). Patients were provided with the Zephyr BioHarness 3.0 device and were instructed to start wearing it after waking up in the morning and shutting it down before going to sleep, for four days. Glycemia of the patients was recorded with an iPro2 Professional CGM sensor, which takes a measurement of plasma glucose levels every 5 minutes, in the same four days in which ECG was recorded. [26]

Table 1 – Information collected at patient enrollment. To preserve the anonymity of the patients the clinical information is not linked with the signals in the dataset and only the range of the clinical data are reported.

Age	Gender	Height(cm)	Weight (kg)
NA	Man	180–189	80–89
20–29	Man	170–179	60–69
20–29	Man	180–189	70–79
20–29	Man	180–189	80–89
30–39	Man	180–189	80–89
30–39	Man	190–199	70–79
30–39	Woman	160–169	70–79
60–69	Woman	150–159	50–59
70–79	Woman	160–169	50–59

8.1.2 Zephyr BioHarness 3.0

Zephyr BioHarness 3.0 (Figure 8.1) is a wearable monitoring system that allows to detect some vital parameters of the patient while carrying out various activities; it is not bulky, it is not invasive, and it is often used for scientific research. The device stores and transmits vital sign data including ECG taken with a I lead sensor (consisting of two silver-coated nylon electrodes working on skin contact) at a rate of 250 Hz and up to 54.89 mV, HR, breathing rate, body position and activity. The BioHarness 3.0 provides the facility to detect and transmit I lead ECG signals to be received by Bluetooth/USB qualified ECG instruments. The device consists of a chest strap equipped with electrodes and textile sensors worn at the level of the chest, and an electronic module called the BioHarness Module attached to the chest strap. The built-in sensors are: two passive sensors in the internal part of the strap to detect ECG signals through conductive pads, a pressure sensor pad in the strap on the subject's left hand side to detect expansion of the rib cage due to breathing action, an internal triaxial accelerometer in the BioHarness Module to measure the subject activity level and the orientation of the device (subject standing, supine, prone, inverted), and a thermistor to measure the device internal temperature.

Figure 8.1 - Zephyr BioHarness 3.0.

The data, after being acquired by sensors, are filtered and recorded in the internal memory of the system or directly sent to a processing system. Zephyr can work in transmitting mode, that is the collected data are transmitted to the processing system via Bluetooth, or can work in transmitting and logging mode, that is the collected data are stored in the system's internal memory and transmitted. In the BioHarness the HR signal is obtained from the filtering of the ECG signal, it is measured in bpm with a resolution of 1 bpm, with a minimum value of 25 bpm and a maximum of 240 bpm. The breathing rate is measured in breaths per minute (BPM) with a resolution of 0.1 BPM, the minimum value is 3 BPM and the maximum 70 BPM. In certain positions of the torso this signal can be subject to artifacts because of the sensor not being adhered to the skin. The temperature is measured in Celsius degrees (°C) with a resolution of 0.1 °C, the minimum value is 10 °C and the maximum 60 °C. The posture is obtained from the processing of accelerometer data and measures the inclination of the subject, in degrees, with respect to the vertical (0°) with values between ± 90°, with a resolution of 1°. A positive value indicates the forward inclination of the subject, while a negative value indicates a backward inclination. Using the triaxial accelerometer, the device removes the effect of gravity and can determine whether the individual is lying down or standing, providing information on what the person is doing. The subject's motor activity is detected by averaging the acceleration module along the three directions in the previous second. The measurement unit is the Vector Magnitude Units (VMU); the data has a resolution of 0.01 VMU and has a minimum value of 0 VMU and a maximum of 16 VMU. The BioHarness Module is powered by an internal rechargeable lithium polymer cell, it is positioned inside a receptacle connected to the chest strap and turns on and off by pressing the front of the device, where there are a series of flashing LEDs that indicate its operating status. The BioHarness Module (Figure 8.2) is recharged

by placing it inside a charging base connected to the PC through a USB port and it is powered with a voltage of 5 V. [27] [28] [29]

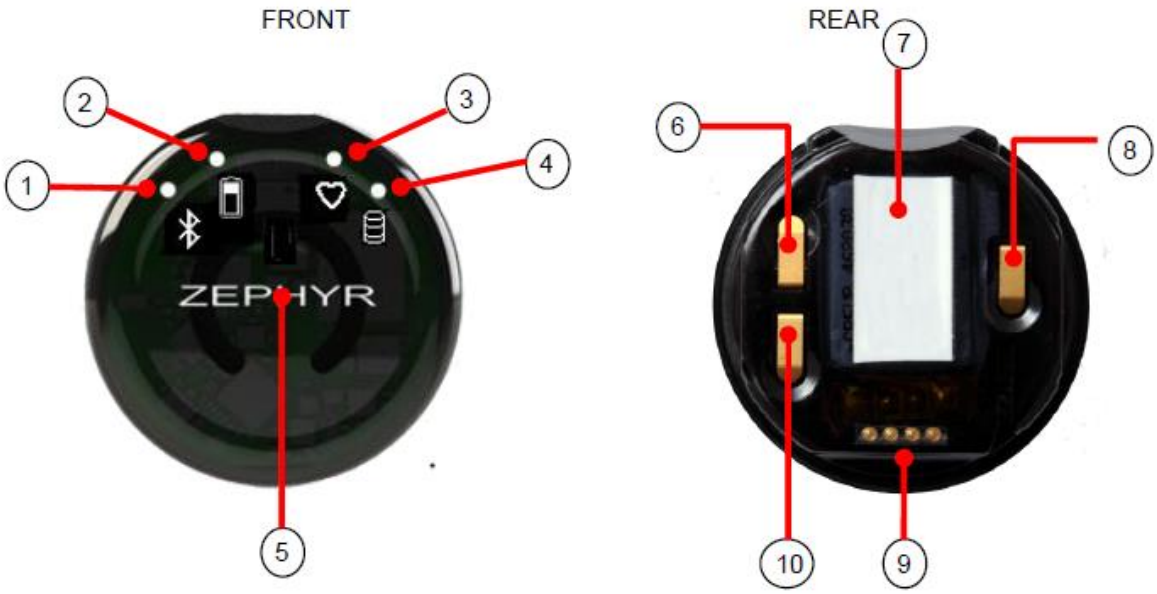

Figure 8.2 – BioHarness Module, front and rear. 1 is the blue Bluetooth indicator LED, 2 is the orange battery indicator LED, 3 is the red HR detection status LED, 4 is the green logging indicator LED, 5 is the ON/OFF button, 6 is the ground spring contact, 7 is the rear label location, 8 is the ECG signal spring contact, 9 is the USB charging/configuration contacts, 10 is the breathing signal spring contact.

The BioHarness chest strap is shown in Figure 8.3.

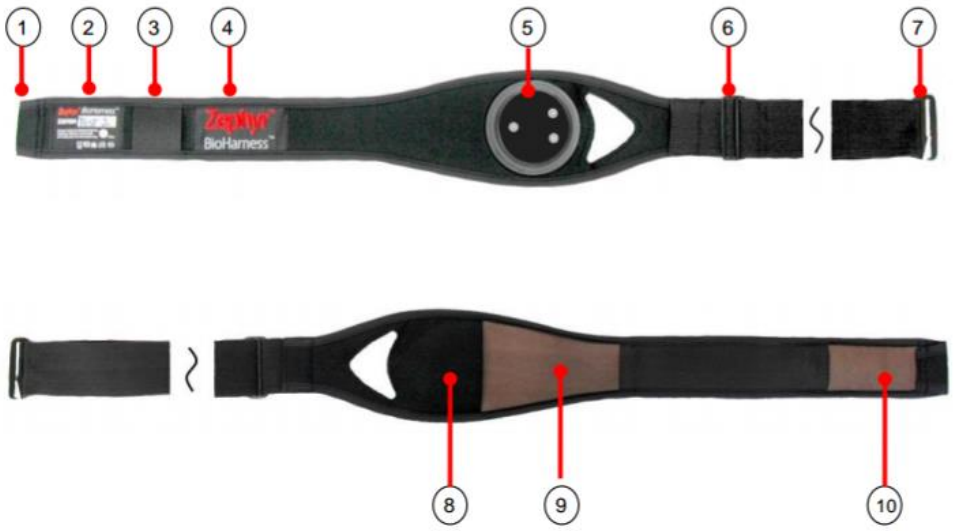

Figure 8.3 – BioHarness chest strap, front and rear. 1 is the main fastener sleeve, 2 is the wash, size and serial # label, 3 is the loop for optional shoulder strap, 4 is the Zephyr brand label, 5 is the BioHarness module receptacle and sensor contacts, 6 is the size adjustment slider buckle, 7 is the main fastener hook, 8 is the internal breathing sensor location, 9 is the conductive ECG sensor pad, 10 is the second conductive ECG sensor pad. [29]

8.1.3 iPro2 Professional CGM

The iPro2 Professional CGM is a small, lightweight, and watertight CGM system that records glucose readings every five minutes. The iPro2 measurements reveal glucose fluctuations that the classic glucometer can miss, allowing a better glucose control. The sensor remains on the patient for 6-7 days while he lives its everyday life; after this time the doctor downloads the data and analyzes the results obtaining a personalized report. The iPro2 CGM system components are: iPro2 recorder, the Enlite sensor, and the Enlite serter (Figure 8.4). The iPro2 Enlite sensor measures glucose in the fluid surrounding the cells of the tissues called interstitial fluid (Figure 8.5) using an enzymatic system, associated with a conversion system that transforms the variations of glucose levels in the body in digital electronic signals of intensity proportional to the concentration of glucose. The iPro2 recorder must be charged into the docking station before it can be used; the docking station must be connected via an USB cable to a wall powered adapter. Once fully charged, after 8 hours, the green light on the docking station will remain on (Figure 8.6).

Figure 8.4 - The iPro2 CGM system components.

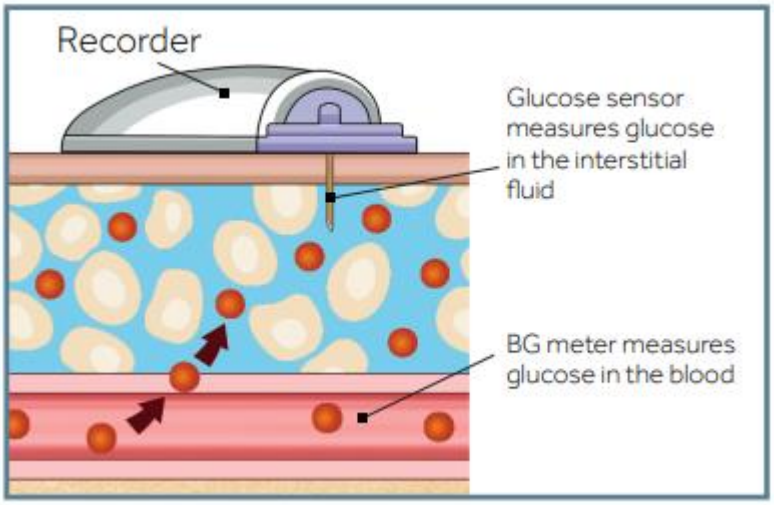

Figure 8.5 – iPro2 Recorder and the Enlite sensor.

Figure 8.6 – The components required for charging the iPro2 CGM: the iPro2 Recorder, the docking station, the USB cable, and the wall powered adapter.

The insertion site of the iPro2 CGM system must be a fatty area free from scar tissue, not restricted by clothing, two inches from the navel, one inch from any insulin injection site, and one inch above belt line.

For the positioning of the iPro2 CGM system the procedure to be followed is the present (Figure 8.7):

- Line up the sensor with the serter and push the serter down until hearing a click.
- Put fingers on each pedestal arm and pull the serter straight up.
- The sensor is now inside the serter and ready for insertion.
- Place the serter against the skin, press and release the bump on the green button.
- Press and hold in the green button.
- Pull the serter away while holding the button.

- Use one hand to hold the sensor against the body and use the other hand to pull needle housing straight out.
- Pull the lower flap of paper straight out to remove the paper backing.
- Pull out the adhesive tab under the sensor connector.
- Apply tape.
- Connect the iPro2 Recorder.
- Remove blue strip paper liner on adhesive tab. Fold adhesive tab over and onto recorder.

Then the patient logs in “iPro2 myLog App” and he can log blood glucose levels acquired with a glucometer, meals, medications, and activity. The data recorded by the iPro2 recorder are downloaded by the doctor that now is able to study the glycemia fluctuations so as to be able to limit them. [30]

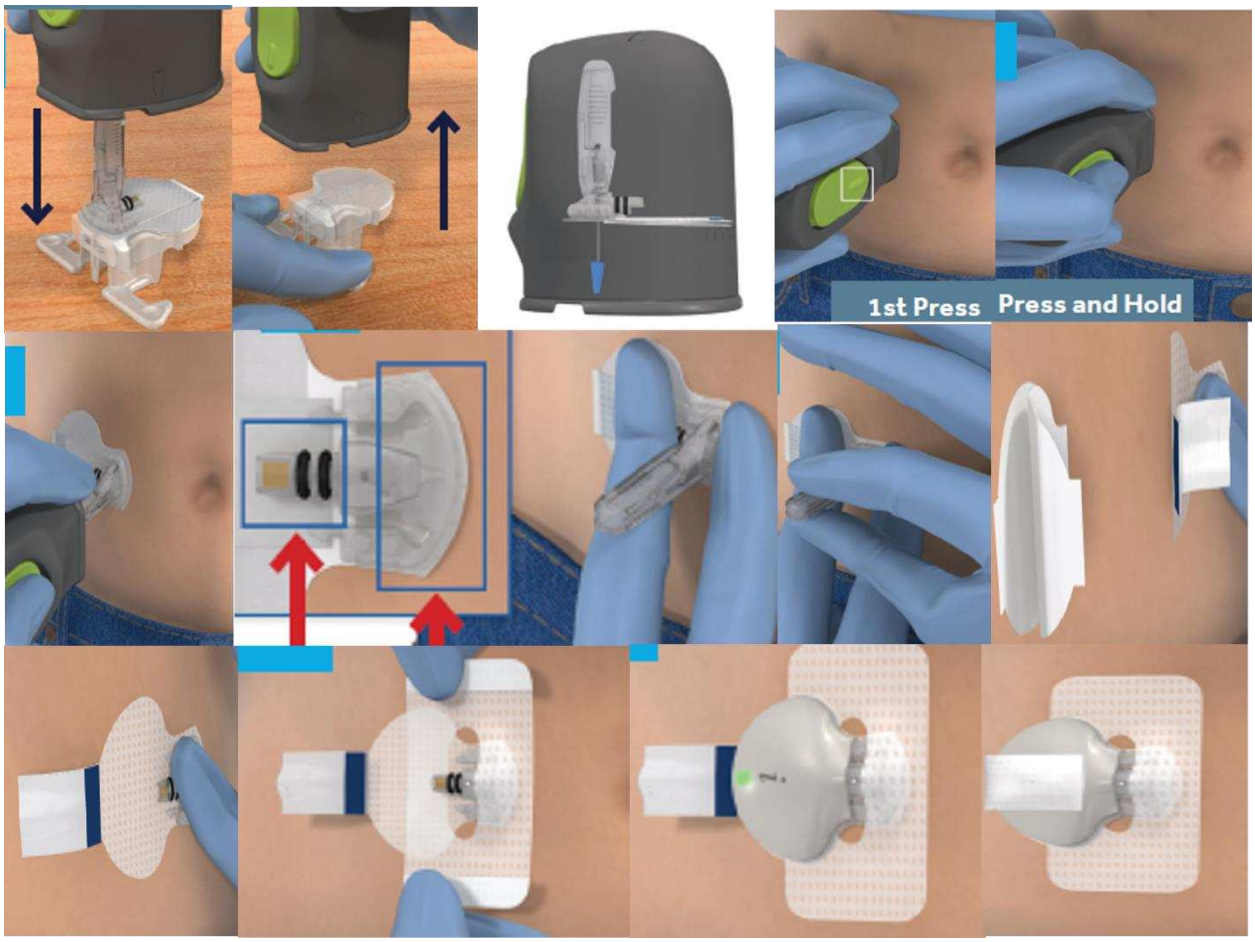

Figure 8.7 – The procedure to be followed for the positioning of the iPro2 CGM system.

8.1.4 Analysis of electrocardiograms and glycemic tracings

The data analyzed in this study are the ECGs acquired by the Zephyr BioHarness 3.0 in the four days of recording and the glycemic tracings recorded by iPro2 Professional CGM in the same four days. The analysis of the ECGs of the 9 subjects recorded for all four days was carried out with the MATLAB R2020a program. Initially the ECGs were divided into shorter windows of ~1 hour and 7 minutes each (corresponding to 1000000 rows in the excel file with ECG data), thus facilitating the visual analysis of the ~450 hours of recording. All these ECG windows were filtered to remove noise provoked by subjects' movements, measurement noise, power line and other disturbances. First the mean of the ECG windows was removed, then the signals were resampled at 200 Hertz, and a third-order band-pass Butterworth filter with cut-off frequency of 0.5 and 40 Hertz was applied. Subsequently these ECG windows were plotted and through visual analysis were classified in this way: in gray the windows in which the recorded ECG was very noisy and not suitable for HRV analysis, in red the windows in which Zephyr had only recorded noise and no ECG was present, in orange the windows in which there were no 5 consecutive minutes of ECG because they were interspersed with noise, in yellow the windows in which there were at least 5 consecutive minutes of ECG, and in green the windows in which the ECG was correctly recorded for throughout the window. Also, glycemic tracings were incomplete or lacking in some of the four days. Then the analysis was restricted to the subjects presenting at least one day with both glycemic tracings and ECG recordings and not only noise. For the subjects presenting more than one day with both glycemic tracings and ECG recording, was selected the day with the highest number of ECG segments without noise and the highest number of CGM data. Then, from the selected day of each subject, all the 5-minutes ECG segments in which the ECG was visible and suitable for the calculation of the HRV parameters were cut and saved, while the parts of the signals in which the classic ECG pattern was not recognizable were discarded. Then all the 5-minutes ECG segments were given in input to the HRVTool by Marcus Vollmer, a software developed as a Matlab Graphical User Interface to compute a list of HRV parameters.

8.1.5 HRVTool

HRVTool is an open-source toolbox with an intuitive and user-friendly interface (Figure 8.8) that allows to perform the analysis of HRV on MATLAB. HRVTool requires in input RR intervals or the ECG waveform and the sampling frequency of the signal. The upper panel of the interface allows the visualization of the RR intervals, of the R peaks, and of the ECG waveform. It is also possible to visualize a particular period of the signal that is given in input to the program, it is possible to remove misplaced R peaks and to reposition them with the buttons “remove” and “add”, it is possible to align beats to the closest minimum or maximum peak, and it is possible to zoom in, zoom out, drag, and select data. There is a filter that removes artifacts such as missing or misplaced R peaks. In the left panel there are the HRV parameters computed by the toolbox following the guidelines of the “Task Force of The European Society of Cardiology and The North American Society of Pacing and Electrophysiology”, and these are SDNN, RMSSD, pNN50, TRI, TINN, ApEn, SD1, SD2, SD1/SD2, LF power, HF power, LF/HF, and HR [31]. HRV measurements are reported into two columns, global column shows HRV parameters computed on the entire signal given in input to the toolbox, while local column shows HRV parameters computed in the time period defined in the upper panel. In the center of the interface there is the local return map that returns the RR intervals, and each point corresponds to a pair of successive intervals. In the right part of the panel it is shown the tachogram, so the RR intervals in function of time, and the spectrum of the tachogram. In the lower panel on the left it is shown the chronological sequence of HR and the local HRV parameters (HRV measures of the last 60 heart beats), while in the lower panel on the right it is shown the return map also called Poincarè plot of the absolute RR intervals (predecessor versus successor). [32] [33]

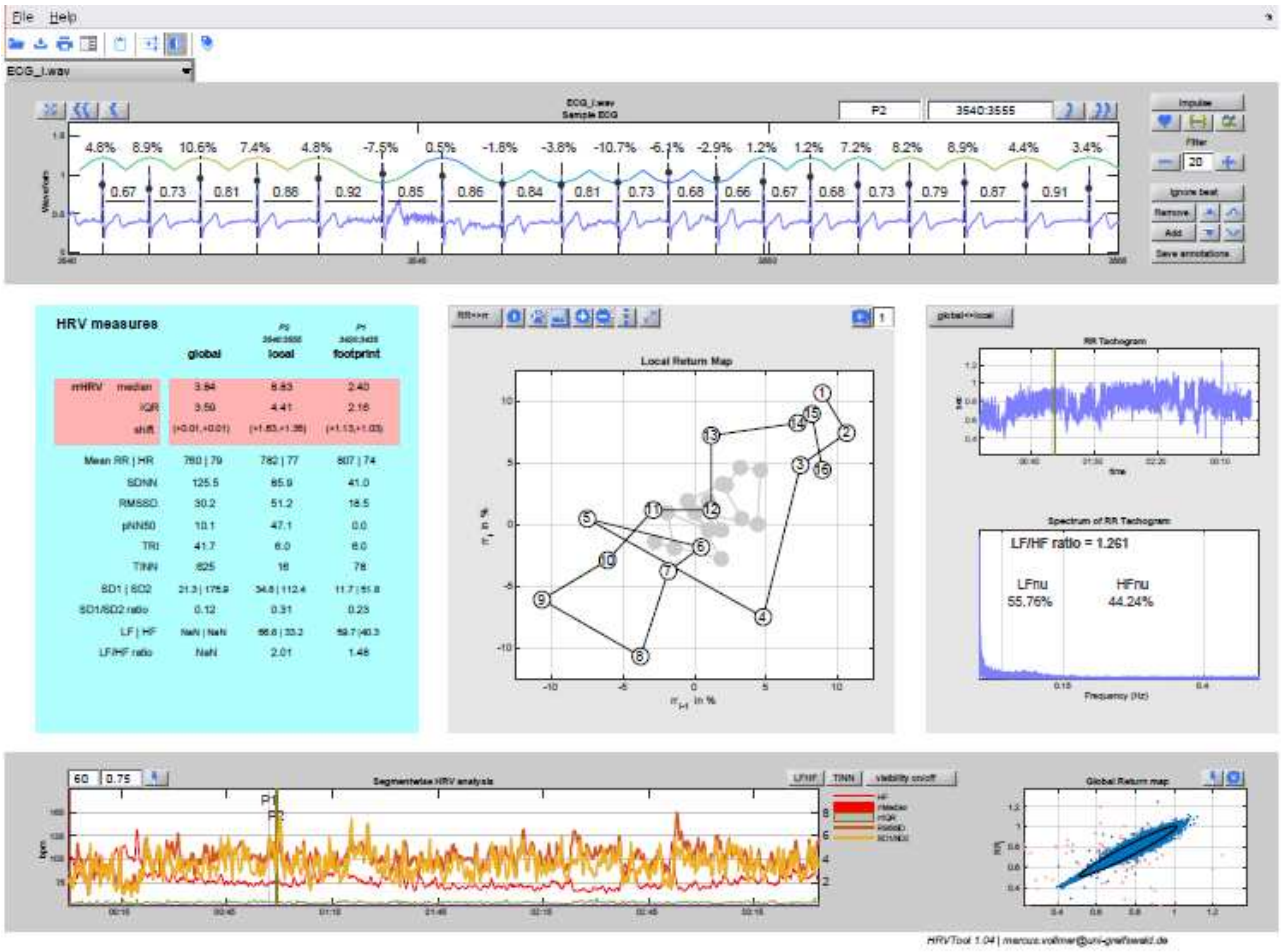

Figure 8.8 – The user-friendly interface of HRVTool. [32]

8.1.6 Statistical analysis

Once SDNN, RMSSD, pNN50, TRI, TINN, ApEn, SD1, SD2, SD1/SD2, LF power, HF power, LF/HF, and HR values were obtained for each of the 5-minutes ECG segments given as input to HRVTool, the Pearson's correlation coefficient (r) was used to study the strength of the correlation between each HRV parameter and the glycemia value recorded in the same 5 minutes in each subject and considering all the subjects grouped. Statistical significance was set at $p<0.05$.

8.2 Results

In Table 2, Table 3, Table 4, Table 5, Table 6, Table 7, Table 8, Table 9, and Table 10 it is possible to observe details of ECG classification in terms of data present or missing for each window, day, and subject. Table 11 shows details of glycemic tracings classification in terms of data present or missing for each day and each subject.

Table 2 - Details of ECG classification in terms of data present or missing for each window and day of subject 1. In gray are reported the windows in which the recorded ECG is very noisy and not suitable for HRV analysis, in red the windows in which Zephyr has only recorded noise and no ECG is present, in orange the windows in which there are no 5 consecutive minutes of ECG because they are interspersed with noise, in yellow the windows in which there are at least 5 consecutive minutes of ECG, and in green the windows in which the ECG is correctly recorded for throughout the window.

SUBJECT 1			
DAY 1	DAY 2	DAY 3	DAY 4
10:09:39 - 11:16:19	10:56:44 - 12:03:24	06:36:24 - 07:43:04	06:34:57 - 07:41:37
11:16:19 - 12:22:59	12:03:24 - 13:10:04	07:43:04 - 08:49:44	07:41:37 - 08:48:17
12:22:59 - 13:29:39	13:10:04 - 14:16:44	08:49:44 - 09:56:24	08:48:17 - 09:54:57
13:29:39 - 14:36:19	14:16:44 - 15:23:24	09:56:24 - 11:03:04	09:54:57 - 11:01:37
14:36:19 - 15:42:59	15:23:24.- 16:30:04	11:03:04 - 12:09:44	11:01:37 - 12:08:17
15:42:59 - 16:49:39	16:30:04- 17:36:44	12:09:44 - 13:16:24	12:08:17 - 13:14:57
16:49:39 - 17:56:19	17:36:44 - 18:43:24	13:16:24 - 14:23:04	**13:14:57 - 13:48:01**
17:56:19 - 19:02:59	18:43:24- 19:50:04	14:23:04 - 15:29:44	
19:02:59- 20:09:39	19:50:04 - 20:56:44	15:29:44 - 16:36:24	
20:09:39 - 21:16:19	**20:56:44 - 21:41:04**	16:36:24 - 17:43:04	
21:16:19 - 22:22:59		17:43:04 - 18:49:44	
22:22:59 - 22:23:26		**18:49:44 - 19:19:59**	

Table 3 - Details of ECG classification in terms of data present or missing for each window and day of subject 2. In gray are reported the windows in which the recorded ECG is very noisy and not suitable for HRV analysis, in red the windows in which Zephyr has only recorded noise and no ECG is present, in orange the windows in which there are no 5 consecutive minutes of ECG because they are interspersed with noise, in yellow the windows in which there are at least 5 consecutive minutes of ECG, and in green the windows in which the ECG is correctly recorded for throughout the window.

SUBJECT 2			
DAY 1	DAY 2	DAY 3	DAY 4
12:35:54 - 13:42:34	06:44:21 - 07:51:01	06:33:20 - 07:40:00	07:01:03 -08:07:43
13:42:34 - 14:49:14	07:51:01 - 08:57:41	07:40:00 - 08:46:40	08:07:43 - 09:14:23
14:49:14 - 15:55:54	08:57:41 - 10:04:21	08:46:40 - 09:53:20	09:14:23 - 10:21:03
15:55:54 - 17:02:34	10:04:21 - 11:11:01	09:53:20 - 11:00:00	10:21:03 - 11:27:43
17:02:34 - 18:09:14	11:11:01 - 12:17:41	11:00:00 - 12:06:40	11:27:43 - 12:34:23
18:09:14 - 19:15:54	12:17:41- 13:24:21	12:06:40 - 13:13:20	12:34:23 - 13:41:03
19:15:54 - 20:18:15	13:24:21 - 14:31:01	**13:13:20 - 13:39:45**	13:41:03 - 14:47:43
	14:31:01 - 15:37:41	14:06:08 - 15:12:48	14:47:43 - 15:54:23
	15:37:41 - 16:44:21	15:12:48 - 16:19:28	**15:54:23 - 16:46:39**
	16:44:21 - 17:51:01	16:19:28 - 17:26:08	17:43:12 - 18:49:52
	17:51:01 - 18:57:41	17:26:08 - 18:32:48	18:49:52 - 19:56:32
	18:57:41 - 20:00:53	18:32:48 - 19:39:28	**19:56:32 - 20:09:23**
		19:39:28 - 20:25:57	

Table 4 - Details of ECG classification in terms of data present or missing for each window and day of subject 3. In gray are reported the windows in which the recorded ECG is very noisy and not suitable for HRV analysis, in red the windows in which Zephyr has only recorded noise and no ECG is present, in orange the windows in which there are no 5 consecutive minutes of ECG because they are interspersed with noise, in yellow the windows in which there are at least 5 consecutive minutes of ECG, and in green the windows in which the ECG is correctly recorded for throughout the window.

SUBJECT 3			
DAY 1	DAY 2	DAY 3	DAY 4
06:00:57 - 07:07:37	09:24:32 - 10:31:12	00:54:40 - 02:01:20	05:33:24 - 06:40:04
07:07:37 - 08:14:17	10:31:12 - 11:37:52	02:01:20 - 03:08:00	06:40:04 - 07:46:44
08:14:17 - 09:20:57	11:37:52 - 12:44:32	03:08:00 - 04:14:40	07:46:44 - 08:53:24
09:20:57 - 10:27:37	12:44:32 - 13:51:12	**04:14:40 - 04:56:11**	08:53:24 - 10:00:04
10:27:37 - 11:34:17	13:51:12 - 14:57:52	18:06:15 - 19:12:55	10:00:04 - 11:06:44
11:34:17 - 12:40:57	14:57:52 - 16:04:32	19:12:55 - 20:19:35	11:06:44 - 12:13:24
12:40:57 - 13:47:37	16:04:32- 17:11:12	20:19:35 - 21:26:15	12:13:24 - 13:20:04
13:47:37 - 14:54:17	17:11:12 - 18:17:52	**21:26:15 - 21:31:46**	13:20:04 - 14:26:44
14:54:17 - 16:00:57	18:17:52 - 19:24:32		**14:26:44 - 15:17:31**
16:00:57 - 17:07:37	19:24:32 - 20:31:12		
17:07:37 - 18:14:17	20:31:12 - 21:37:52		
18:14:17 - 19:20:57	21:37:52 - 22:44:32		
19:20:57 - 20:27:37	22:44:32 - 23:51:12		
20:27:37 - 21:34:17	**23:51:12 - 00:54:40**		
21:34:17 - 22:12:22			

Table 5 - Details of ECG classification in terms of data present or missing for each window and day of subject 4. In gray are reported the windows in which the recorded ECG is very noisy and not suitable for HRV analysis, in red the windows in which Zephyr has only recorded noise and no ECG is present, in orange the windows in which there are no 5 consecutive minutes of ECG because they are interspersed with noise, and in yellow the windows in which there are at least 5 consecutive minutes of ECG.

SUBJECT 4			
DAY 1	DAY 2	DAY 3	DAY 4
06:55:10 - 08:01:50	07:21:06 - 08:27:46	08:05:42 - 09:12:22	06:32:58 - 07:39:38
08:01:50 - 09:08:30	08:27:46 - 09:34:26	09:12:22 - 10:19:02	07:39:38 - 08:46:18
09:08:30 - 10:15:10	09:34:26 - 10:41:06	10:19:02 - 11:25:42	08:46:18 - 09:52:58
10:15:10 - 11:21:50	10:41:06 - 11:47:46	11:25:42 - 12:32:22	09:52:58 - 10:59:38
11:21:50 - 12:28:30	11:47:46- 12:54:26	12:32:22 - 13:39:02	10:59:38 - 12:06:18
12:28:30 - 13:35:10	12:54:26 - 14:01:06	13:39:02 - 14:45:42	12:06:18 - 13:12:58
13:35:10 - 14:41:50	14:01:06 - 15:07:46	14:45:42 - 15:52:22	13:12:58 - 14:19:38
14:41:50 - 15:48:30	15:07:46 - 16:14:26	**15:52:22 - 16:07:19**	14:19:38 - 15:26:18
15:48:30 - 16:55:10	16:14:26 - 17:21:06		15:26:18 - 16:32:58
16:55:10 - 18:01:50	17:21:06 - 18:27:46		**16:32:58 - 16:49:30**
18:01:50 - 18:36:12	18:27:46 - 19:34:26		**16:49:30 - 17:45:56**
19:33:00 - 19:58:35	**19:34:26 - 19:39:54**		

Table 6 - Details of ECG classification in terms of data present or missing for each window and day of subject 5. In red are reported the windows in which Zephyr has only recorded noise and no ECG is present, in orange the windows in which there are no 5 consecutive minutes of ECG because they are interspersed with noise, and in yellow the windows in which there are at least 5 consecutive minutes of ECG.

SUBJECT 5			
DAY 1	DAY 2	DAY 3	DAY 4
10:27:42 - 10:29:37	09:23:58 - 10:30:38	08:42:25 - 09:49:05	08:02:17 - 09:08:57
10:40:51 - 11:47:31	10:30:38 - 11:37:18	09:49:05 - 10:55:45	09:08:57 - 10:15:37
11:47:31 - 12:54:11	**11:37:18 - 11:40:30**	10:55:45 - 12:02:25	10:15:37 - 11:22:17
12:54:11 - 14:00:51	11:40:30 - 12:47:10	12:02:25 - 13:09:05	11:22:17 - 12:28:57
14:00:51 - 15:07:31	12:47:10 - 13:53:50	13:09:05 - 14:15:45	12:28:57 - 13:35:37
15:07:31 - 16:14:11	13:53:50 - 15:00:30	14:15:45 - 15:22:25	13:35:37 - 14:42:17
16:14:11 - 17:20:51	15:00:30 - 16:07:10	15:22:25 - 16:29:05	**14:42:17 - 15:22:24**
17:20:51 - 18:27:31	16:07:10 - 17:13:50	16:29:05 - 17:35:45	
18:27:31 - 19:34:11	17:13:50 - 18:20:30	17:35:45 - 18:42:25	
19:34:11 - 20:40:51	18:20:30 - 19:27:10	18:42:25 - 19:49:05	
20:40:51 - 21:47:31	19:27:10 - 20:33:50	19:49:05 - 20:55:45	
21:47:31 - 22:27:27	20:33:50 - 21:40:30	20:55:45 - 22:02:25	
	21:40:30 - 22:47:10	**22:02:25 - 22:45:41**	
	22:47:10 - 23:02:25		

Table 7 - Details of ECG classification in terms of data present or missing for each window and day of subject 6. In red are reported the windows in which Zephyr has only recorded noise and no ECG is present, in orange the windows in which there are no 5 consecutive minutes of ECG because they are interspersed with noise, in yellow the windows in which there are at least 5 consecutive minutes of ECG, and in green the windows in which the ECG is correctly recorded for throughout the window.

SUBJECT 6			
DAY 1	DAY 2	DAY 3	DAY 4
06:46:44 - 07:53:24	08:03:53 - 09:10:33	08:57:56 - 10:04:36	10:30:26 - 11:37:06
07:53:24 - 09:00:04	09:10:33 - 10:17:13	10:04:36 - 11:11:16	11:37:06 - 12:43:46
09:00:04 - 10:06:44	10:17:13 - 11:23:53	11:11:16 - 12:17:56	12:43:46 - 13:50:26
10:06:44 - 11:13:24	11:23:53 - 12:30:33	12:17:56 - 13:24:36	13:50:26 - 14:57:06
11:13:24 - 12:20:04	**12:30:33 - 12:48:31**	13:24:36 - 14:31:16	14:57:06 - 16:03:46
12:20:04 - 13:26:44	15:13:03 - 16:19:43	14:31:16 - 15:37:56	16:03:46 - 17:10:26
13:26:44 - 14:33:24	16:19:43 - 17:26:23	15:37:56 - 16:44:36	17:10:26 - 18:17:06
14:33:24 - 15:08:04	17:26:23 - 18:33:03	16:44:36 - 17:51:16	18:17:06 - 19:23:46
15:08:04 - 16:14:44	18:33:03 - 19:39:43	17:51:16 - 18:57:56	19:23:46 - 20:30:26
16:14:44 - 17:21:24	19:39:43 - 20:46:23	18:57:56 - 20:04:36	20:30:26 - 21:37:06
17:21:24 - 18:28:04	**20:46:23 - 21:34:25**	20:04:36 - 21:11:16	**21:37:06 - 21:57:07**
18:28:04 - 19:34:44		21:11:16 - 22:17:56	
19:34:44 - 20:41:24		**22:17:56 - 22:54:40**	
20:41:24 - 21:48:04			
21:48:04 - 22:54:44			
22:54:44 - 00:01:24			
00:01:24 - 01:08:04			
01:08:04 - 02:11:34			

Table 8 - Details of ECG classification in terms of data present or missing for each window and day of subject 7. In red are reported the windows in which Zephyr has only recorded noise and no ECG is present, in orange the windows in which there are no 5 consecutive minutes of ECG because they are interspersed with noise, in yellow the windows in which there are at least 5 consecutive minutes of ECG, and in green the windows in which the ECG is correctly recorded for throughout the window.

SUBJECT 7			
DAY 1	DAY 2	DAY 3	DAY 4
08:42:43 - 09:49:23	07:52:44 - 08:59:24	06:46:57 - 07:53:37	08:27:21 - 09:34:01
09:49:23 - 10:56:03	08:59:24 - 10:06:04	07:53:37 - 09:00:17	09:34:01 - 10:40:41
10:56:03 - 12:02:43	10:06:04 - 11:12:44	09:00:17 - 10:06:57	10:40:41 - 11:47:21
12:02:43 - 13:09:23	11:12:44 - 12:19:24	10:06:57 - 11:13:37	11:47:21 - 12:54:01
13:09:23 - 14:16:03	12:19:24 - 13:26:04	11:13:37 - 12:20:17	12:54:01 - 14:00:41
14:16:03 - 15:22:43	13:26:04 - 14:32:44	12:20:17 - 13:26:57	14:00:41 - 15:07:21
15:22:43 - 16:29:23	14:32:44 - 15:39:24	13:26:57 - 14:33:37	15:07:21 - 16:14:01
16:29:23 - 17:36:03	15:39:24 - 16:46:04	14:33:37 - 15:40:17	16:14:01 - 17:20:41
17:36:03 - 18:42:43	16:46:04 - 17:52:44	15:40:17 - 16:46:57	17:20:41 - 18:27:21
18:42:43 - 19:49:23	**17:52:44 - 18:45:07**	16:46:57 - 17:53:37	18:27:21 - 19:34:01
19:49:23 - 20:56:03		17:53:37 - 19:00:17	19:34:01 - 20:40:41
20:56:03 - 22:02:43		19:00:17 - 20:06:57	20:40:41 - 21:47:21
22:02:43 - 23:09:23		20:06:57 - 21:13:37	**21:47:21 - 22:09:08**
23:09:23 - 23:46:17		21:13:37 - 22:20:17	
		22:20:17 - 23:26:57	
		23:26:57 - 00:33:37	
		00:33:37 - 01:40:17	
		01:40:17 - 02:40:48	

Table 9 - Details of ECG classification in terms of data present or missing for each window and day of subject 8. In red are reported the windows in which Zephyr has only recorded noise and no ECG is present, in orange the windows in which there are no 5 consecutive minutes of ECG because they are interspersed with noise, in yellow the windows in which there are at least 5 consecutive minutes of ECG, and in green the windows in which the ECG is correctly recorded for throughout the window.

SUBJECT 8		
DAY 1	DAY 2	DAY 3
06:43:00 - 07:49:40	10:13:52 - 11:20:32	10:51:39 - 11:58:19
07:49:40 - 08:56:20	11:20:32 - 12:27:12	11:58:19 - 13:04:59
08:56:20 - 10:03:00	12:27:12 - 13:33:52	13:04:59 - 14:11:39
10:03:00 - 11:09:40	13:33:52 - 14:40:32	14:11:39 - 15:18:19
11:09:40 - 12:16:20	14:40:32 - 15:47:12	15:18:19 - 16:24:59
12:16:20 - 13:23:00	15:47:12 - 16:53:52	16:24:59 - 17:31:39
13:23:00 - 14:29:40	16:53:52 - 18:00:32	17:31:39 - 18:38:19
14:29:40 - 15:36:20	18:00:32 - 19:07:12	18:38:19 - 19:44:59
15:36:20 - 16:43:00	19:07:12 - 20:13:52	19:44:59 - 20:51:39
16:43:00 - 17:49:40	20:13:52 - 21:20:32	20:51:39 - 21:58:19
17:49:40 - 18:56:20	21:20:32 - 22:27:12	**21:58:19 - 22:54:51**
18:56:20 - 20:03:00	22:27:12 - 23:33:52	22:54:51 - 00:01:31
20:03:00 - 21:09:40	23:33:52 - 00:40:32	00:01:31 - 01:08:11
21:09:40 - 22:04:09	00:40:32 - 01:47:12	01:08:11 - 02:14:51
	01:47:12 - 02:53:52	02:14:51 - 03:21:31
	02:53:52 - 03:26:30	03:21:31 - 04:28:11
		04:28:11 - 05:34:51
		05:34:51 - 06:41:31
		06:41:31 - 07:48:11
		07:48:11 - 08:05:09

Table 10 - Details of ECG classification in terms of data present or missing for each window and day of subject 9. In red are reported the windows in which Zephyr has only recorded noise and no ECG is present, and in yellow the windows in which there are at least 5 consecutive minutes of ECG.

SUBJECT 9			
DAY 1	DAY 2	DAY 3	DAY 4
05:59:30 - 07:06:10	06:14:52 - 07:21:32	08:21:59- 09:28:39	09:09:29 - 10:16:09
07:06:10 - 08:12:50	07:21:32 - 08:28:12	09:28:39 - 10:35:19	10:16:09 - 11:22:49
08:12:50 - 09:19:30	08:28:12 - 09:34:52	10:35:19 - 11:41:59	11:22:49 - 12:29:29
09:19:30 - 10:26:10	09:34:52 - 10:41:32	11:41:59 - 12:48:39	12:29:29 - 13:36:09
10:26:10 - 11:32:50	10:41:32 - 11:48:12	12:48:39 - 13:55:19	13:36:09 - 14:42:49
11:32:50 - 12:39:30	11:48:12 - 12:54:52	13:55:19 - 15:01:59	**14:42:49 - 15:03:37**
12:39:30 - 13:46:10	12:54:52 - 14:01:32	15:01:59 - 16:08:39	15:03:37 - 16:10:17
13:46:10 - 14:52:50	14:01:32 - 15:08:12	16:08:39 - 17:15:19	16:10:17 - 17:16:57
14:52:50 - 15:59:30	15:08:12 - 16:14:52	17:15:19 - 18:21:59	17:16:57 - 18:23:37
15:59:30 - 17:06:10	16:14:52 - 17:21:32	18:21:59 - 19:28:39	18:23:37 - 19:30:17
17:06:10 - 18:12:50	17:21:32 - 18:28:12	**19:28:39 - 20:09:48**	19:30:17 - 20:36:57
18:12:50 - 18:45:56	18:28:12 - 19:34:52		20:36:57 - 21:43:37
	19:34:52 - 20:39:14		**21:43:37 - 22:45:44**

Table 11 - Details of glycemic tracings classification in terms of data present or missing for each day and each subject: in green are reported the days in which CGM is registered and in red the days in which CGM is lacking.

SUBJECT 1	SUBJECT 2	SUBJECT 3
day 1	day 1	day 1
day 2	day 2	day 2
day 3	day 3	day 3
day 4	day 4	day 4
SUBJECT 4	SUBJECT 5	SUBJECT 6
day 1	day 1	day 1
day 2	day 2	day 2
day 3	day 3	day 3
day 4	day 4	day 4
SUBJECT 7	SUBJECT 8	SUBJECT 9
day 1	day 1	day 1
day 2	day 2	day 2
day 3	day 3	day 3
day 4	day 4	day 4

Therefore, the analysis was restricted to subjects 2, 3, 4, 6, 7, 8, presenting at least one day with both glycemic tracings and ECG recording and not only noise. The 5-minutes segments of ECG used for HRV parameters computation were extracted from subject 2 day 3, subject 3 day 1, subject 4 day 1, subject 6 day 2, subject 7 day 1, and subject 8 day 2, presenting the highest number of ECG segments without noise and the highest number of CGM data, for a total of 327 5-minutes ECG segments. The HRV parameters obtained by HRVTool relative to subject 4 were unrealistic (an example is the HR that remained always constant at 46 bpm for the entire duration of the registration), so subject 4 was discarded from the statistical analysis. Table 12 shows the resultant r(p) between each HRV parameter computed on 5-minutes ECG segments and the glycemia values recorded in the same 5 minutes for each subject.

Table 12: Correlation between HRV and glycemia in each subject represented as r (p).

	SUBJECT 2	SUBJECT 3	SUBJECT 6	SUBJECT 7	SUBJECT 8
	GLYCEMIA	GLYCEMIA	GLYCEMIA	GLYCEMIA	GLYCEMIA
SDNN	0.2038 (0.1900)	0.7978 (0.0552)	-0.2775 (0.0790)	0.1642 (0.2310)	-0.0165 (0.8444)
RMSSD	-0.0661 (0.6734)	-0.2399 (0.2588)	-0.2599 (0.1008)	0.1769 (0.1964)	-0.1388 (0.0970)
pNN50	-0.0101 (0.9489)	-0.3914 (0.0586)	-0.2659 (0.0929)	**0.4826 (0.0002)**	**-0.1953 (0.0190)**
TRI	0.1812 (0.2449)	0.0926 (0.6668)	-0.2691 (0.0889)	**0.3677 (0.0058)**	-0.1046 (0.2121)
TINN	0.1187 (0.4484)	0.2166 (0.3092)	-0.2443 (0.1237)	**0.3103 (0.0211)**	-0.0903 (0.2815)
ApEn	-0.1732 (0.2667)	-0.0550 (0.7987)	**-0.3724 (0.0165)**	0.1047 (0.4467)	0.0649 (0.4400)
SD1	-0.0662 (0.6734)	-0.2400 (0.2586)	-0.2599 (0.1008)	0.1769 (0.1965)	-0.1389 (0.0969)
SD2	0.2289 (0.1398)	0.0882 (0.6818)	-0.2934 (0.0627)	0.1570 (0.2522)	-0.0010 (0.9908)
SD1/SD2	-0.1648 (0.2909)	**-0.4296 (0.0362)**	**-0.3656 (0.0187)**	0.1093 (0.4270)	**-0.2078 (0.0124)**
LF power	0.1901 (0.2221)	**0.4111 (0.0459)**	**0.3664 (0.0185)**	0.2266 (0.0962)	**0.2523 (0.0023)**
HF power	-0.1901 (0.2221)	**-0.4111 (0.0459)**	**-0.3664 (0.0185)**	-0.2266 (0.0962)	**-0.2523 (0.0023)**
LF/HF	0.2804 (0.0686)	**0.4380 (0.0323)**	**0.3988 (0.0098)**	0.2505 (0.0651)	0.1490 (0.0746)
HR	0.1910 (0.2199)	**0.4787 (0.0180)**	**0.4289 (0.0051)**	**-0.3999 (0.0025)**	-0.0114 (0.8918)

In Figure 8.9, Figure 8.10, Figure 8.11, Figure 8.12, Figure 8.13, Figure 8.14, Figure 8.15, Figure 8.16, Figure 8.17, Figure 8.18, Figure 8.19, Figure 8.20, Figure 8.21, it is represented the correlation between each HRV parameter computed on all 5-minutes ECG segments and the glycemia values recorded in the same 5 minutes considering all the subjects grouped.

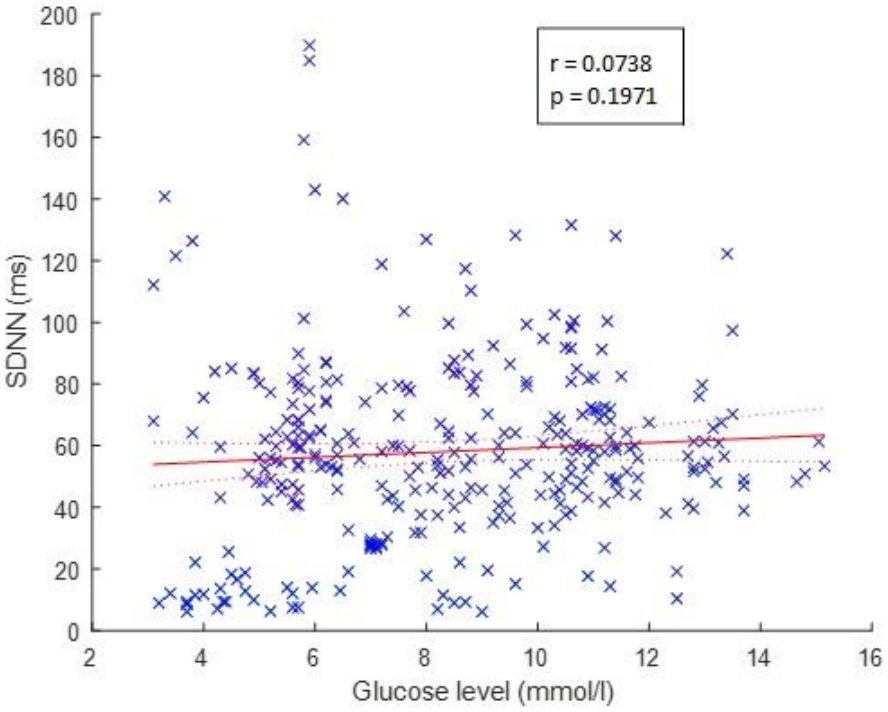

Figure 8.9- Correlation between SDNN and glycemia values considering all the subjects grouped. In red it is shown the regression line. r and p are also shown.

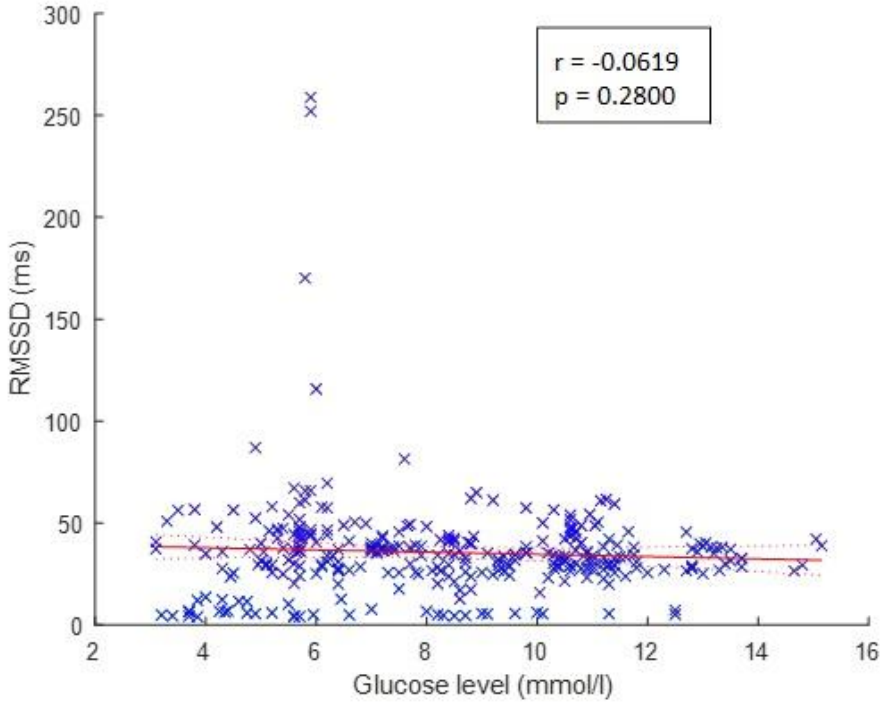

Figure 8.10 - Correlation between RMSSD and glycemia values considering all the subjects grouped. In red it is shown the regression line. r and p are also shown.

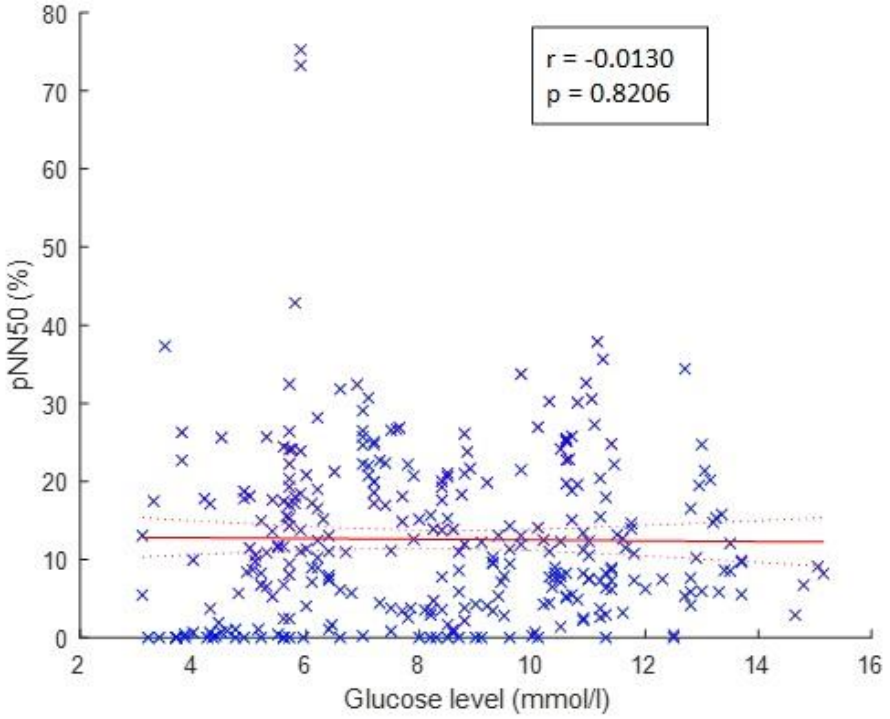

Figure 8.11 - Correlation between pNN50 and glycemia values considering all the subjects grouped. In red it is shown the regression line. r and p are also shown.

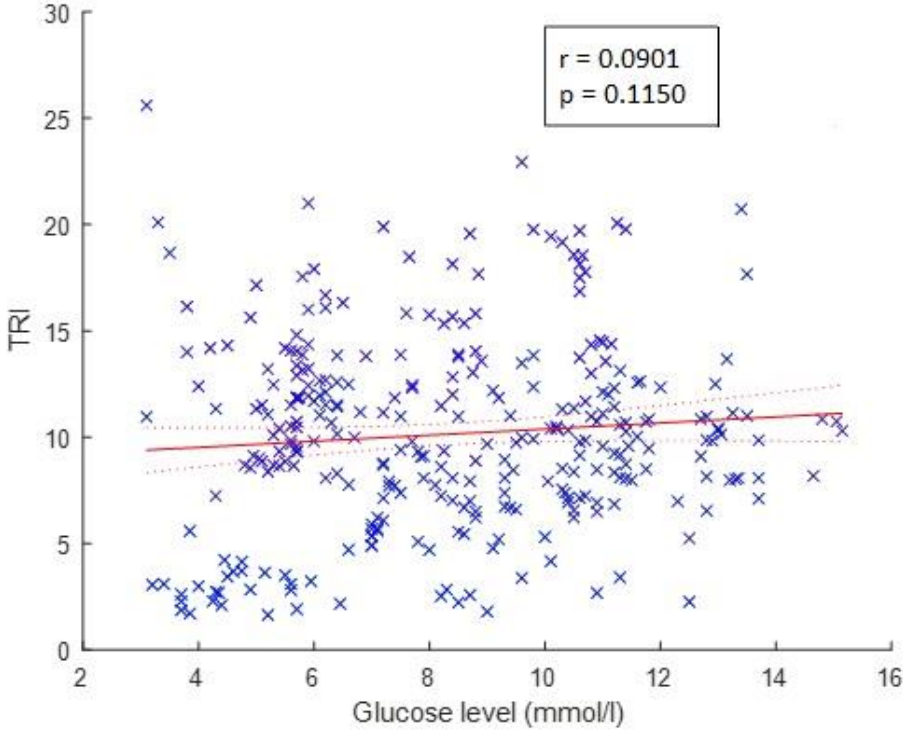

Figure 8.12 - Correlation between TRI and glycemia values considering all the subjects grouped. In red it is shown the regression line. r and p are also shown.

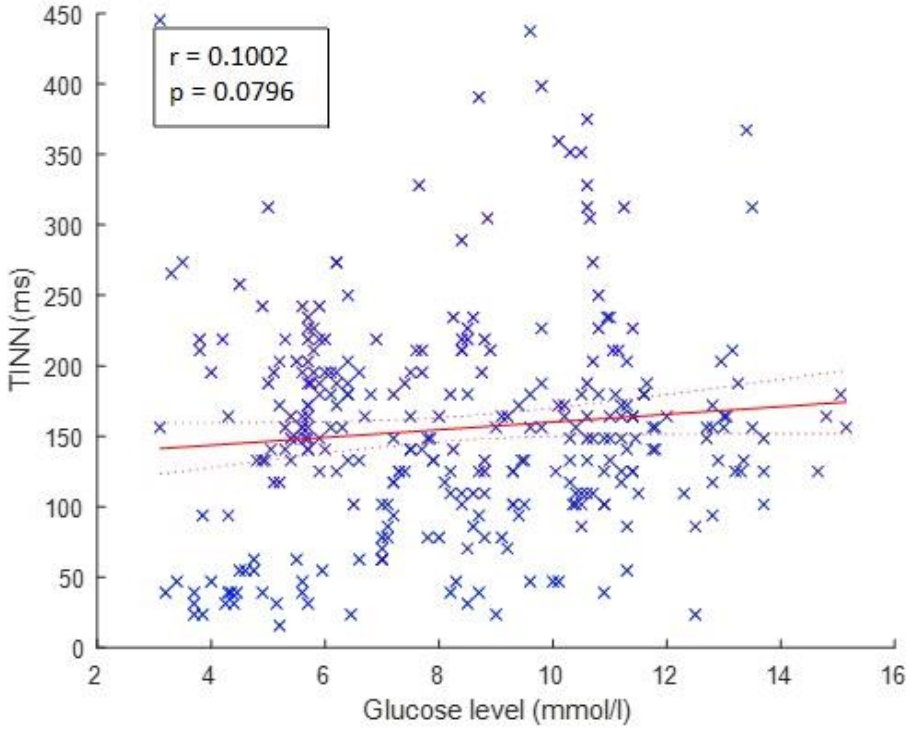

Figure 8.13 - Correlation between TINN and glycemia values considering all the subjects grouped. In red it is shown the regression line. r and p are also shown.

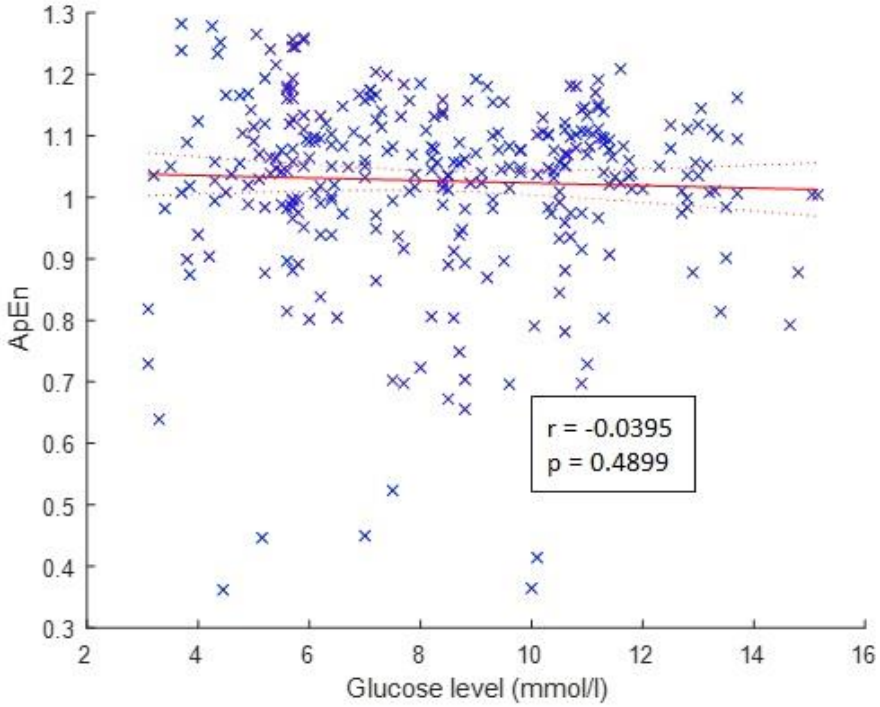

Figure 8.14 - Correlation between ApEn and glycemia values considering all the subjects grouped. In red it is shown the regression line. r and p are also shown.

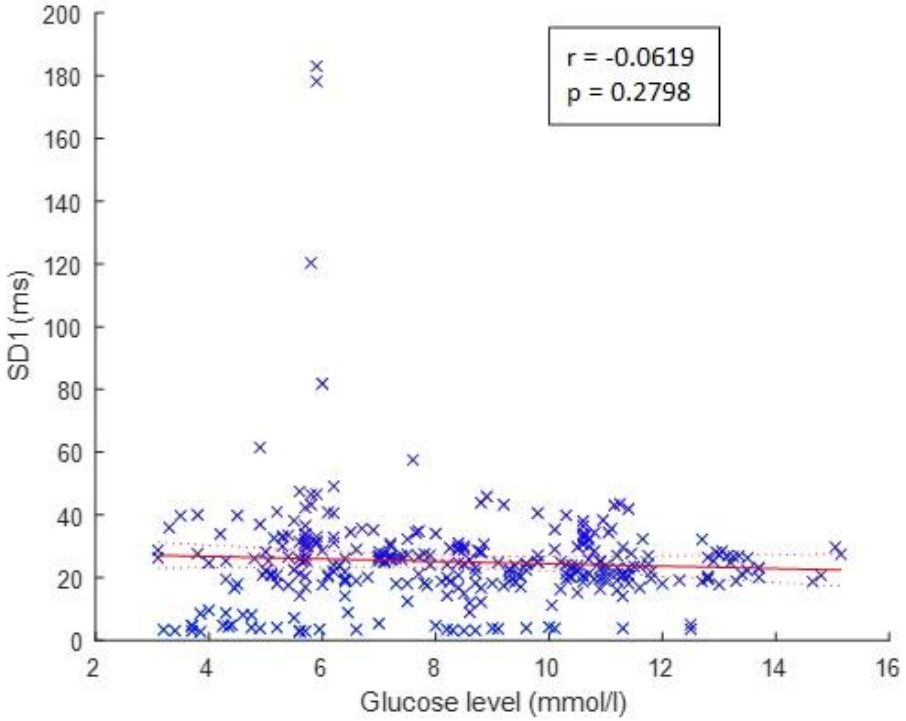

Figure 8.15- Correlation between SD1 and glycemia values considering all the subjects grouped. In red it is shown the regression line. r and p are also shown.

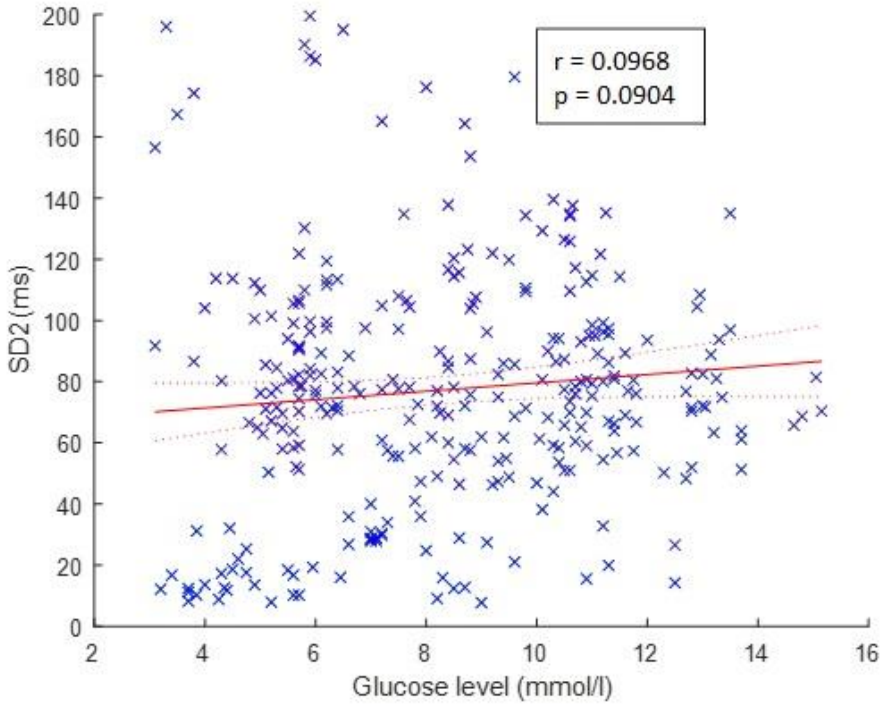

Figure 8.16 - Correlation between SD2 and glycemia values considering all the subjects grouped. In red it is shown the regression line. r and p are also shown.

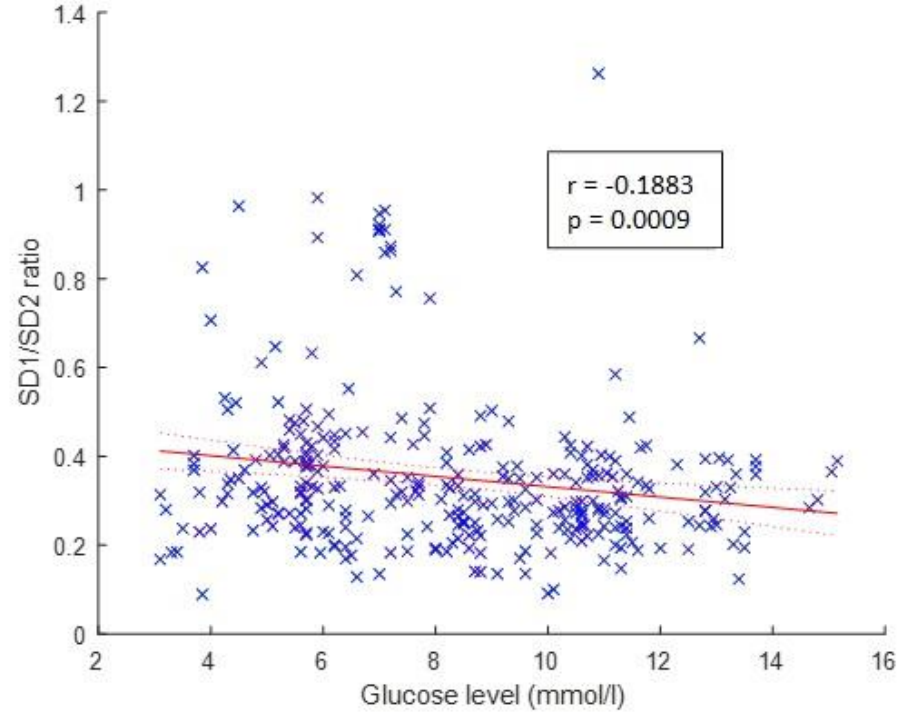

Figure 8.17 - Correlation between SD1/SD2 and glycemia values considering all the subjects grouped. In red it is shown the regression line. r and p are also shown.

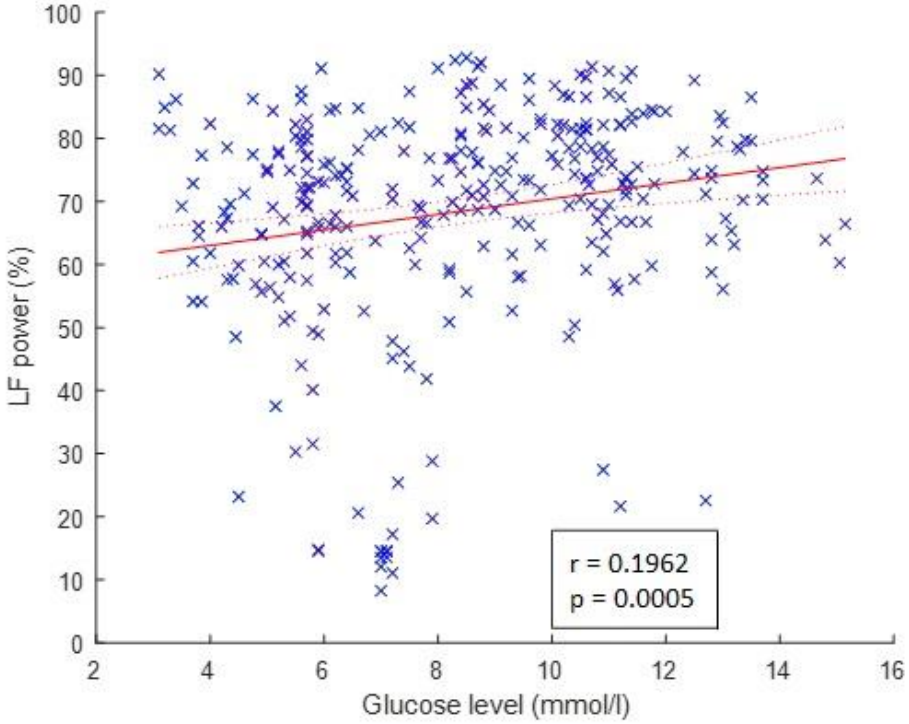

Figure 8.18 - Correlation between LF power and glycemia values considering all the subjects grouped. In red it is shown the regression line. r and p are also shown.

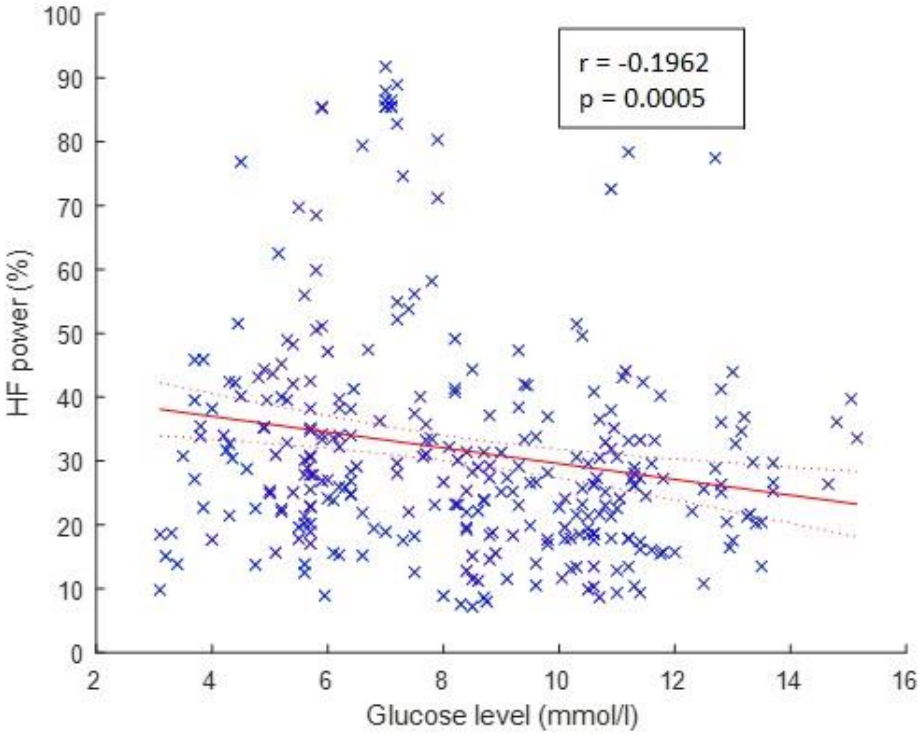

Figure 8.19 - Correlation between HF power and glycemia values considering all the subjects grouped. In red it is shown the regression line. r and p are also shown.

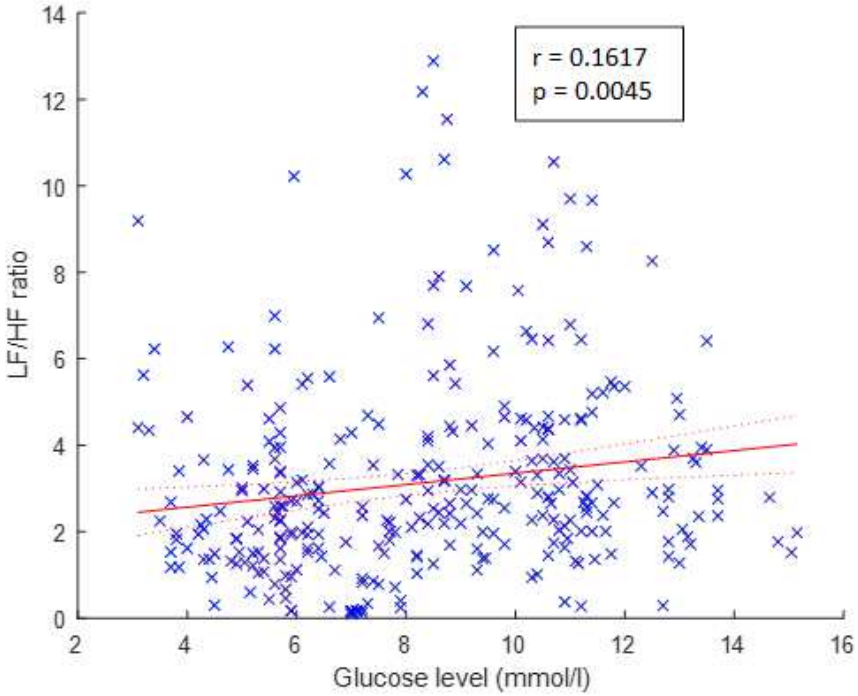

Figure 8.20 - Correlation between LF/HF and glycemia values considering all the subjects grouped. In red it is shown the regression line. r and p are also shown.

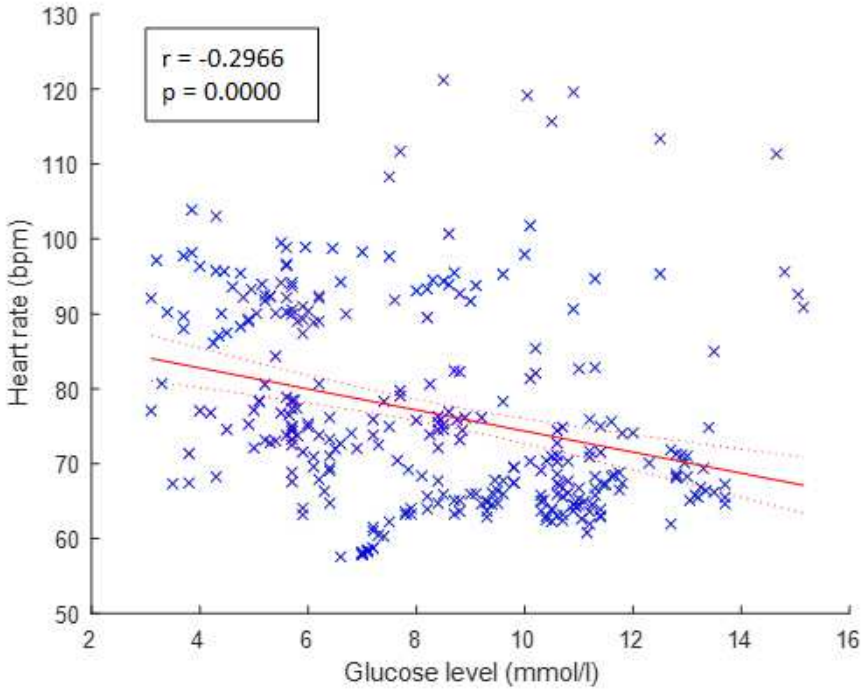

Figure 8.21 - Correlation between HR and glycemia values considering all the subjects grouped. In red it is shown the regression line. r and p are also shown.

Discussion and conclusions

The aim of this study was to assess the relationship between HRV parameters computed in 5-minutes intervals and glycemia values in the same 5-minutes, in a population of subjects affected by type 1 DM while carrying out activities of daily living. The dataset used is publicly available and composed of 9 patients with type 1 DM monitored for four days with the wearable device Zephyr BioHarness3.0 for ECG recording and with iPro2 CGM system for glycemia measurements. From Table 12, reporting for each subject the correlations between HRV parameters computed in 5-minutes ECG intervals and blood glucose levels measured in the same 5 minutes, it is visible that the highest number of significant correlations and the strongest correlations are present in subject 3 and subject 6; these correlations are between glycemia and: SD1/SD2, LF power, HF power, LF/HF, and HR. While the correlation between glycemia and SDNN is positive in subjects 2, 3, and 7, it is negative in subjects 6 and 8. Similarly the correlations between glycemia and: RMSSD, pNN50, TRI, TINN, ApEn, SD1, SD2, SD1/SD2, and HR are positive or negative when observed in different subjects. Conversely, the correlations between glycemia and LF power and between glycemia and LF/HF are positive for all the subjects studied, while the correlation between glycemia and HF power is negative for all the subjects observed. From Figure 8.9, Figure 8.10, Figure 8.11, Figure 8.12, Figure 8.13, Figure 8.14, Figure 8.15, Figure 8.16, Figure 8.17, Figure 8.18, Figure 8.19, Figure 8.20, Figure 8.21, it is clear that there are no strong correlations between HRV parameters computed in 5-minutes ECG intervals and blood glucose levels measured in the same 5 minutes considering all the subjects grouped. Weak but significant correlations are highlighted between blood glucose and: SD1/SD2, LF power, HF power, LF/HF, and HR. The non-significant correlations found are between glycemia and: SDNN, RMSSD, pNN50, TRI, TINN, ApEn, SD1, and SD2. In this study, SDNN, that is a quantification of the total HRV and reflets both sympathetic and parasympathetic nervous system activity on the heart, appears to be positively correlated with blood glucose, contrary to what was found in the study by Nguyen et al. [17], Singh et al. [19], and Vishinov et al. [8]. RMSSD, reflecting mainly the parasympathetic nervous system activity on the heart, is negatively correlated with glycemia values, in accordance with the study by Nguyen et al. [17]. Furthermore, while in the present study LF power, reflecting sympathetic nervous system activity on the heart, is positively correlated with blood glucose, a negative

correlation was found in the studies by Nguyen et al. [17], Rothberg et al. [20], and Singh et al. [19]. HF power, reflecting parasympathetic nervous system activity on the heart, appears to be negatively correlated with glycemic values in accordance with the findings of Nguyen et al. [17], Rothberg et al. [20] and Singh et al. [19]. Also pNN50, reflecting parasympathetic nervous system activity on the heart, appears to be negatively correlated with glycemic values, in agreement with the results of Nguyen et al. [17]. LF/HF ratio, which reflects the balance between sympathetic and parasympathetic nervous system activity, appears to be positively correlated with blood glucose contrary to the findings of Nguyen et al. [17] and Singh et al. [19] but in agreement with Rothberg et al. [20]. SD1/SD2, measuring the unpredictability of the RR time series, is negatively correlated with glycemia contrary to what Vishinov et al. [8] found. SD2, TRI and TINN are weakly and positively correlated with blood glucose values while SD1 and ApEn are negatively correlated with glycemia. HR has a negative correlation with blood glucose values as demonstrated by Nguyen et al. [21]. The correlations between HRV parameters and glycemia studied here are for the most part weak and not always in agreement with the literature. It is likely that the cause of this disagreement with the literature's findings lies in the non-standardization of the activities performed by the subjects during the day, since practicing more or less intense physical activity, eating a non-standardized meal, and following one's daily routine, can affect HRV and glycemia values, thus altering the correlations results. Instead, in the studies in literature, the ECGs were recorded in the hospital and while the subjects were at rest, and the glycemic values were measured fasting or after a well-defined period of time from the last meal which was also standardized, or the measurements were made while the subjects were sleeping. These studies, carried out in controlled environments and in a standardized way, do not reflect the patient's daily living conditions; therefore, they constitute only a partial view of the relationship between HRV and glycemia, hence cannot be used to deduce glycemic values starting from HRV. So, it is interesting to study the correlation between HRV and glycemia in every-day life conditions because the results reflect more the reality. In this study, subjects wear Zephyr Bioharness 3.0 without the help of an assistant and therefore the quality of the recorded ECG signal is not high but has noise and motion artifacts, making the signal analysis complex and making it difficult to identify the ECG R peaks by HRVTool. As shown from Table 2 to Table 10, the ECG acquisition is not successful for long periods of time, however it is not a surprising result since the chest strap equipped with electrodes and textile sensors can lose contact with the skin during physical movements; furthermore, if the textile sensors are

not correctly humidified the signal is not acquired. In conclusion, from this study it emerges the existence of weak correlations between HRV parameters computed in 5-minutes intervals and glycemia values in the same 5-minutes in a population of subjects affected by type 1 DM while carrying out activities of daily living. Although the correlations found are not strong and only some are significant, this study may represent an important starting point that paves the way for possible future studies aiming at estimate glycemia values from HRV obtained from the ECG recorded through non-invasive wearable sensors.

Bibliography

[1] Saladin K.S., “Anatomia & fisiologia”, Piccin, 2011, quinta edizione.

[2] Stanfield C.L., "Principles of Human Physiology", Pearson, Medical Journal of Australia., 2012, fifth edition.

[3] Saladin K.S., “Anatomy & Physiology”, Piccin, 2011, fifth edition.

[4] Koeppen B.M., Stanton B.A., “Berne & Levy Physiology”, Elsevier, 2018, seventh edition.

[5] Branca F.P., “Fondamenti di Ingegneria Clinica”, volume 1, Springer, 2000, first edition.

[6] Goldberger J. J., Ng J., “Practical Signal and Image Processing in Clinical Cardiology”, Springer, 2010, first edition.

[7] Shaffer F., Ginsberg J.P., “An Overview of Heart Rate variability Metrics and Norms”, 2017 5(September):1–17.

[8]Vishinov I., Gusev M., Member S., Vavlukis M., Poposka L., “Correlating Short-Term Heart Rate Variability and Instantaneous Blood Glucose Measurements”, 2020.

[9] Park D., Lee M., Park S.E., Seong J., Youn I., “Determination of Optimal Heart Rate Variability Features Based on SVM-Recursive Feature Elimination for Cumulative Stress Monitoring Using ECG Sensor”, Sensors, 2018.

[10] Società Italiana di Diabetologia, “Automonitoraggio glicemico” https://www.siditalia.it/divulgazione/autocontrollo-glicemico

[11] Perrone F., Lamberti C., “Dispositivi per l’assistenza “home care” dei pazienti diabetici”, Alma Mater Studiorum Università di Bologna, 2015.

[12] Suh S. and Kim J. H., “Glycemic variability: How do we measure it and why is it important?,” Diabetes Metab. J., vol. 39, no. 4, pp. 273–282, 2015, doi: 10.4093/dmj.2015.39.4.273.

[13] Bragd J., Adamson U., Ba¨cklund L. B., Lins P. E., Moberg E., Oskarsson P., “Can glycaemic variability, as calculated from blood glucose self-monitoring, predict the development of complications in type 1 diabetes over a decade?” Diabetes Metab 2008;34:612–6.

[14] Frontoni S., Di Bartolo P., Avogaro A., Bosi E., Paolisso G., and Ceriello A., “Glucose variability: An emerging target for the treatment of diabetes mellitus,” Diabetes Res. Clin. Pract., vol. 102, no. 2, pp. 86–95, 2013, doi: 10.1016/j.diabres.2013.09.007.

[15] Piersanti A., Giurato F., Burattini L., Tura A., and Morettini M., “Comparison of software packages for the analysis of continuous glucose monitoring data,” 2021 IEEE Int. Symp. Med. Meas. Appl. MeMeA 2021 - Conf. Proc., pp. 1–6, 2021, doi: 10.1109/MeMeA52024.2021.9478698.

[16] Millard L. A. C., Patel N., Tilling K., Lewcock M., Flach P. A., and Lawlor D. A., “Software application profile: GLU: A tool for analysing continuously measured glucose in epidemiology,” bioRxiv, 2018, doi: 10.1101/500256.

[17] Nguyen L., Su S., Nguyen H.T., “Effects of Hyperglycemia on Variability of RR, QT and corrected QT intervals in Type 1 Diabetic Patients”, 2013.

[18] Kudat H., Akkaya V., Sozen A. B., Salman S., Demirel S., Ozcan M., Atilgan D., Yilmaz M. T., Guven O., “Heart rate variability in diabetes patients”, J Int Med Res, vol. 34, pp. 291-6, 2006.

[19] Singh J.P., Larson M. G., O’Donnell C. J., Wilson P. F., Tsuji H., Lloyd-Jones D. M., Levy D., "Association of hyperglycemia with reduced heart rate variability (The Framingham Heart Study)," The American journal of cardiology, vol. 86, pp. 309-312, 2000.

[20] Rothberg L.J., Lees T., Clifton-Bligh R., Lal S. “Association Between Heart Rate Variability Measures and Blood Glucose Levels: Implications for Noninvasive Glucose Monitoring for Diabetes”, Diabetes Technology & Therapeutics VOL. 18, NO. 6

[21] Nguyen L., Su S., Nguyen H.T., Member S. “Identification of Hypoglycemia and Hyperglycemia in Type 1 Diabetic Patients Using ECG Parameters”, 2012;2716–9.

[22] Stein P.K., Barzilay J.I., Domitrovich P.P., “The relationship of heart rate and heart rate variability to non-diabetic fasting glucose levels and the metabolic syndrome : The Cardiovascular Health Study”, 2007.

[23] Coopmans C., Zhou T.L., Henry R.M.A., Heijman J., Schaper N.C., Van Der Kallen C.J.H., “ Both Prediabetes and Type 2 Diabetes Are Associated With Lower Heart Rate Variability: The Maastricht Study”, 2020;43(May):1126–33.

[24] E. Lespagnol et al., “In amateur athletes with type 1 diabetes, a 9-day period of cycling at moderate-to-vigorous intensity unexpectedly increased the time spent in hyperglycemia, which was associated with impairment in heart rate variability,” Diabetes Care, vol. 43, no. 10, pp. 2564–2573, 2020, doi: 10.2337/dc19-1928.

[25] V. V. Klimontov, N. E. Myakina, and N. V. Tyan, “Heart rate variability is associated with interstitial glucose fluctuations in type 2 diabetic women treated with insulin,” Springerplus, vol. 5, no. 1, 2016, doi: 10.1186/s40064-016-1932-z.

[26] Dubosson F., Ranvier J.E., Bromuri S., Calbimonte J.P., Ruiz J., Schumacher M., "The open D1NAMO dataset: A multi-modal dataset for research on non-invasive type 1 diabetes management" Informatics Med Unlocked. 2018;13(October):92–100.

[27] Pisano E., Lamberti DEIS C., Alma Mater Studiorum Università degli Studi di Bologna, Gullà V., Gullà F., Aditech S.r.l., Corsani I., Ciullini G., Manzi V., Bovenzi A., Galanti G., Dipartimento di Medicina dello Sport della Università degli Studi di Firenze, "Il monitoraggio psicofisico".

[28] Pisano E., Lamberti C., Salmon Cinotti T., Alma Mater Studiorum Università di Bologna "Monitoraggio dell'attività motoria mediante dispositivi indossabili", 2010/2011.

[29] Zephyr BioHarness 3.0 User Manual,
https://www.zephyranywhere.com/media/download/bioharness3-user-manual.pdf

[30] iPro2 Step by step training guide,

https://carelink.minimed.com/marcom/ipro2/en/US/iPro2-Step-by-Step-Training-Guide.pdf

[31] Guidelines, T. N. American, and Guidelines, "Guidelines Heart rate variability," Eur. Heart J., vol. 17, pp. 354–381, 1996, doi: 10.1161/01.CIR.93.5.1043.

[32] Vollmer M., "HRVTool - An Open-Source Matlab Toolbox for Analyzing Heart Rate Variability," Comput. Cardiol. (2010)., vol. 2019-September, 2019, doi: 10.23919/CinC49843.2019.9005745.

[33] HRVTool English Manual https://marcusvollmer.github.io/HRV/manual_english.html

Acknowledgments

I would like to thank all those who have been close to me during the writing of the thesis and during these years of university career. Special thanks go to Prof. Burattini, Supervisor of the thesis, to Prof. Morettini, Co-supervisor, and to Dr. Marcantoni. It is thanks to their guidance, their support, and knowledge of the tools they have put at my disposal that this thesis has been realized. I thank my family who encouraged and supported me at all times, especially the most difficult, allowing me to reach this goal. I thank my boyfriend Gianmarco, thank you for being by my side in happy and less happy moments, for sharing the joys and goals and for having listened to me and helped me in difficulties, having you by my side has made me stronger, wiser, and happier. I thank the historical friends with whom I have shared the joy of successes and the disappointment of failures and my colleagues with whom I have shared many projects, emotions, and carefree moments.